We will like to appreciate the time and guidance of the anonymous reviewers whose suggestions have been very helpful during the correction of this manuscript. We have noted all the issues raised and made effort towards improving the clarity, language, length, presentation and other vital points included in your remark. This has guided our decision to focus majorly on the observed irregularity pattern during the equinoxes and hopefully improve on the clarity of the discussion. Hence, the highlighted portion (yellow) which is related to the OLR results has been deleted. We hope that you also consider this as an improvement to the manuscript and we will appreciate further suggestions on improving the quality of this manuscript. Thanks

Referee 1

First about the title "Spread F occurrence features at different longitudinal regions during low and moderate solar activity". I think as the present manuscript describes only RSF so title should be more specific.

a)Thanks for your suggestion. This will be corrected while revising the manuscript

In the line 17-18, "at different…..2013" the meaning is not clear here.

a)This have been changed to *"during 2010 and 2013 which represents the low and moderate solar activity periods respectively"*

3. In lines 24-26, "The observed features ………….of occurrence", please rephrase the sentence.

a) Changed to *"The longitudinal distribution of the RSF occurrence features include the observed difference in the onset time, duration and seasonal occurrence peak"*.

4. Please put a space between the word "widespread" in line number 38.

(a) This has been corrected

5. Line 47-48: "The pre-reversal enhancement (PRE)………..in conjunction" the vertical drift velocity of what and how it is related with PRE?

(a) This has been corrected

6. Line 50-52: please put some references in favor of the statement "The PRE……instability mechanism".

(a) Relevant references have been added as suggested

7. Line 54: replace "of the" with "in".

8. Line 57: use "conditions" instead of "condition"

(a) Both comments (7) and (8) have been corrected as suggested

9. Line 58: whenever you are using the phrase "past studies" please include some suitable references.

(a)Thank you, some relevant references have been included.

10. Lines 59-61: "The complex……….low latitude region." Please include the references Haldoupis et al., (2003) and Miller (1997) a. Haldoupis C, Kelley MC, Hussey GC, Shalimov S. Role of unstable sporadic-E layers in the generation of midlatitude spread F. Journal of Geophysical Research: Space Physics. 2003 Dec;108(A12) b. Miller, C. A, Electrodynamics of midlatitude spread F 2.A new theory of gravity wave electric fields, J. Geophys.Res., 102(A6), 11533-11538, 1997.

(a) Thanks for your suggestion.

11. Line 103-104: “the different………….solar activity”, please mention which seasons you are using for your manuscript, yearly mean of SSN or F(10.7) and the longitudinal range using for this study.

(a) *“the different”* have been changed to *“equinox and solstice”*, while the yearly mean of F(10.7) was included for each year. However, the longitudes of the considered stations have been specified under the methodology section.

12. Line 127: Please specify the longitude range.

(a) The longitudes have already been listed in Table 1. However, we have reframed the sentence.

13. In Table 1, please refer the short forms for all ionosonde stations that you used throughout the manuscript.

(a) Thanks for your suggestion.

14. Line 135: please delete “echo” from the statement “the recorded…..SSF”

(a) Deleted

15. In the same sentence please some references of “Bowman” e.g., a. Bowman, G. G., (1960), A relationship between “spread-F” and the height of the F2 ionospheric layer, Aust. J. Phys., 13, 69-72. b. Bowman, G. G., (1998), Short-term delays (hours) of ionospheric spread F occurrence at a range of latitudes, following geomagnetic activity, J. Geophys.Res., 103(A6), 11627-11634

a) The suggested references have been added

16. Line 139: please replace the word “height” by “altitude” and delete the words “echo” and “axis”.

(a) This have been corrected as suggested.

17. Line 141: “Hereafter, we…….RSF”, if you consider both RSF and SSF as RSF then why are you mentioning SSF separately?

(a) We have rewritten the highlighted comment.

18. Line 151-153: “the data taken………………MSA period. Since ……….. solar flux unit is similar,” Not clear, are you consider both 2009 and 2010 data for LSA and 2011, 2013 data for MSA? Because mixing of 2009 with 2010 data, also 2011 with 2013 data is not a scientific approach to analyze equatorial ionosphere.

(a) Thanks. The data taken during Oct, 2009 (72.14 sfu) was only used to represent the RSF occurrence at this region during the LSA period due to the low data availability during Oct, 2010 (81 sfu) at the Jicamarca station. We assumed that there will be negligible difference between the background ionospheric condition and subsequently the ionospheric parameters driving the spread F initiation at this region during both years. We also observed that Maruyama et al.,(2009) made a similar comparison between ionospheric parameters taken during two equinox seasons (Mar 2005 and Sept 2004) of different years but similar solar flux index (fig.2). Though we are open to corrections and will to adjust the highlighted statement if considered necessary.

19. Line 162-164: “The seasonal variation of RSF……..MSA period”. Please mention the Figure numbers where you have shown the histogram patterns.

a) This sentence have been deleted and the preceding sentence rewritten as

"*Figures 4 and 5 present the hourly distribution of the RSF occurrence percentage across the different longitude sectors during the LSA period and the MSA period, which was averaged over each month based on the available data at these stations."*

20. Line 165-167: "while…………….months" please replace "start" by "starting".

a) This and other related words have been corrected.

21. In the same sentence please mention that the statement you have made is that true for all longitude sectors?

a) This is true and clearly shown in Figure 4 for all longitudes, except the significantly delayed starting time observed at the KWJ station during the June solstice.

22. Line 172-175: "Li et al., (2011)……………LSA year." Where is the highlighted result you have mentioned? The irregularity development at the equatorial region normally initiated around the post-sunset period over the magnetic equator and thereby transported along the magnetic field lines to East ward directions. The post-midnight irregularities are not always the trail of post-sunset irregularities but some fresh irregularity bubbles may develop during late evening hours depending on the nighttime ionospheric effects. So please discuss the statement properly.

a) This statement was based on their Figure 4 and their description of the observed EFI occurrence in the African sector during LSA (page 5, section 3.2). The following was included as you have suggested;

"*The maximum RSF occurrence percentage was mostly observed before the midnight period (around 21:00 LT) during most seasons at each longitude. However, there are months which have a significantly larger RSF occurrence percentage near the midnight than at 21:00 LT. This could be attributed to either the irregularity onset delayed till pre-midnight period as a result of the ionospheric condition or multiple days with irregularities originating from distant location drifting into the ionogram's field of view (Balan et al., 2018; Narayanan et al., 2014).*"

23. Line 176-178: "Furthermore, the…….sunset time." Where is the supporting information against this statement? It can't be concluded just from the histogram plots.

a) Su et al (2009) described the relationship between the delayed zonal drift reversal, peak vertical plasma drift, the instability growth rate and the irregularity onset time at positive magnetic declination longitudes. Their analysis supports our observation at the KWJ station during the June solstice. The field aligned Pedersen conductivity term in the zonal drift velocity equation is considered a major factor influencing the seasonal difference in the zonal drift reversal.

Furthermore, we made a comparison between the average altitudinal variation of the field aligned Pedersen conductivity during the March equinox and October equinox using the TIEGCM model (figure was not included in the manuscript).

24. Figure 4: Please mention in the x axis that the time is taken in Local Time (LT). Also mention the years of observations in the caption.

a) That will be corrected

25. Line 185-186: "ILR station….recorded" 100% of what?

a) This has been changed to *"all the stations except at the ILR station, where the RSF occurrence rate was already ~100 % during the LSA."*

26. Line 195-196: “irregularity onset……onset time,” where is the supporting information regarding this statement?

a) Though supporting information was provided initially in the discussion section but we have included more information as suggested and edited the initial discussion.

Su et al., (2009) analyzed the zonal drift reversal control of the vertical plasma drift, instability growth rate and irregularity onset in the 150^0 *-* 170^0 *longitude range. The relatively small RSF occurrence percentage as observed at this region during the J-solstice of the LSA could be attributed to the zonal drift reversal effect and the weak background ionospheric condition in the region. The zonal drift reversal delay was described as being strongly influenced and indirectly proportional to the field aligned Pedersen conductivity. Hence, an expectedly larger density and a corresponding increase in the field aligned Pedersen conductivity during the MSA will cause an earlier zonal drift reversal and larger occurrence rate as shown in Figure 5.*

27. Line 198-200: “The largest STBA……period”, where is the supporting information against this statement?

a) We having rewritten this part and added supporting information as suggested.

28. Figure 5: Please mention in the x axis that the time is taken in Local Time (LT). Also mention the years of observations in the caption.

a) Thanks, it will be corrected.

29. Line 210-215: “The observed pattern …….. D-solstice period.” How can you conclude that ESF occurrence is independent of solar activity whereas solar activity is one of the major controlling agents of equatorial ionosphere?

a) Thanks for your observation. That was actually a wrong attempt towards highlighting the probable contribution of other factors to the solar flux dependence of RSF occurrence in the region during the S-equinox. However, the statement has been deleted and the preceding statements edited in order to achieve a better illustration of our observation.

30. Line 215: what do you mean by non-occurrence of RSF?

a) This has been changed to “absence of RSF occurrence”

31. Line 218: Please rephrase “anti-solar activity” with “inverse solar activity” throughout the overall manuscript.

a) Thanks. This has been changed

32. Line 219: Please mention the location from where Su et al., (2007) have been described the inverse solar activity effects of RSF events during the solstice seasons.

a) This has been changed to “*The inverse correlation between the solar flux intensity and the RSF occurrence have been observed at the low ESF longitudes from* 230^0 *to* 10^0 *and* 90^0 *to* 260^0 *during the J-solstice and D-solstice respectively (Su et al., 2007)*”

33. Line 226: occurrence percentage of what?

a) Thanks. Corrected to “RSF occurrence percentage”

34. Line 227-229: “The typical ……….ESF events.” Please provide some references in support of your statement.

a) We have added (Dao et al., 2017; Otsuka, 2018).

35. Figure 6: Please mention in the x axis that the time is taken in Local Time (LT).

a) This has been added

36. Line 243: PRE in the equatorial ionosphere normally occurs during sunset or before but not at evening. So please correct the statement in line 243.

a) This has been corrected

37. Line 246-247: "In case of ………………… MSA period." Please mention the proper Figure number in the statement.

a) The statement refers to Figure 7(a and b) and that has been included.

38. Line 252-255: "Such zonal……..sectors", Please put some references.

a) Thanks for your suggestion, (Abdu, 2016; Vichare and Richmond, 2005) have been included.

39. Figure 7 (a and b): Please mention in the x axis that the time is taken in Local Time (LT).

a) That has been corrected

40. Line 285-288: This section is I think not necessary for the manuscript.

a) This section has been deleted as suggested

41. Line 314-316: "The equinox …………. entirely." Please provide some reference.

a) (Manju and Madhav Haridas, 2015; Tsunoda, 2010b) have been added to the sentence.

42. Line 327-329: "They associated ………… On the defined h'FC." Please rephrase the sentence.

a) This sentence has been changed to *"Manju and Madhav Haridas, (2015) explored the probable relationship between the observed equinox asymmetry in the threshold height ($h'F_c$), the ESF occurrence percentage and the O/N_2 ratio."*

43. Line 348-351: "We assume ………………. during both epoch." The meaning of the statement is not clear.

a) Thanks for your suggestion, this section has been changed to;

"This observation is likely due to the complementary role of the major factors influencing the plasma instability growth and their variability with the solar flux intensity. The observed large RSF occurrence percentage during the S-equinox of the LSA at this longitudes have been earlier related to the effect of the contracted ionospheric density. However, the increase in the bottom-side density scale length during the MSA (Lee, 2010) and this will cause an increase in the threshold PRE the irregularity occurrence (Smith et al., 2016)."

44. Line 359: Please replace "longitudes" by "Ionosonde stations".

a) This has been corrected.

45. Figure 8: Please put it in result section instead of discussion.

a) This has been moved to result section as suggested

46. Line 380-401: In my opinion this paragraph is more suitable to demonstrate Figure 8 in result than discussion section.

a) Thanks for your suggestion, this has been moved to result section

47. Line 405-412: "The relationship ……as expressed as V …..." This portion is also not necessary in the discussion section of the present manuscript.

a) This has been removed as suggested

48. Line 413-415: Please make sure the letter front size should be same throughout the whole body of manuscript.

a) This has been corrected

49. Line 417: What is the significance of the dust particles with this study? If you want to keep the statement described in line 417-418, please provide some reference and relate your study with the dust particles.

a) Thanks for your suggestion, this has been removed

<u>Referee 2</u>

1. The authors are requested to highlight what is new in this work.

We have presented an extensive statistical analysis of the RSF occurrence across different longitude sectors during the low and moderate solar activity period. Our results have highlighted and discussed factors contributing to the relevant features observed at these longitudes during the solstice and equinox months, which includes;

The longitudinal variation in the observed equinoctial asymmetry pattern and peak during both epochs.

The anti-solar dependence of the RSF occurrence at the South American sector during the S-equinox season.

This observation and other related analysis presented in our study further highlights the seasonal variation of the ionospheric density as a major factor influencing the observed equinoctial asymmetry in the RSF occurrence.

Apart from providing supporting result to the earlier theorectical analysis of the zonal drift reversal effect to the reduced spread F occurrence percentage at the 150^{o} – 170^{o} longitude range during the June solstice. Our result have also shown that similar asymmetric effect might also exist during the equinoctial seasons of the low solar activity period. Where a significant onset delay and smaller occurrence percentage was observed at the March equinox of the LSA and a corresponding equinoctial asymmetry is observed in the monthly mean vertical plasma drift at this region.

Finally we also analyzed the probable role of the GW from tropospheric source on the observed solstitial asymmetry in the spread F occurrence in the low declination angle longitude region. We have attempted to demonstrate the complementary role of the gravity wave (GW) in the solstitial asymmetry observed at the low declination angle region using OLR measurement as a proxy for the seasonal distribution of the GW activities at each region. We assume your reservation about this approach might be connected with the results from Su et al., (2014). However, a recent study have attributed the poor correlation at some of the regions with the averaging of OLR value over a wide longitude range (Li et al.,2016). Furthermore, our result showed that the suggested approach does not increase the correlation coefficient at CPN. Hence, we have presented a brief analysis of the major factors that could have contributed to the small ESF occurrence percentage at the CPN longitude in spite of the large OLR frequency.

We believe that the presented result and analysis have summarized the prominent features related to the seasonal variation of the irregularity initiation and occurrence across different longitudinal regions. These could provide the relevant to improved empirical modeling of the RSF occurrence distribution.

2. In Fig. 4, one can see high occurrence of Spread F at Ilorin in all seasons, which is clearly different to the other longitudes. No clear discussion can be found in the text. To my point of view, this is a new result and worth to discuss further.

a) Thanks, this has been included in the discussion.

Minor comments:

Pages 13, 15-21: There are several paragraphs with the length more than one page, which made readers confused to understand. Concise description or to divide it in sub-paragraphs will be better.

a) Thanks for your observation. This has been corrected

In Fig 4, the authors showed occurrence rate at Ilorin during Low solar activity. But, in Fig 7, the authors showed monthly averaged virtual height at Ilorin during Medium solar activity. Why they are different period ?

a) Thanks. We will make the necessary correction to the figure caption (Figure 7b should represent the LSA).

Page 18, line 360, “GW”: Gravity waves ?

a) Yes, this was shown in the statement where it first appears.

<u>Referee 3</u>

Major comments:

1. Why the authors consider 2013 as MSA? It is almost the solar maximum of the present solar cycle. It should be HSA, right? For ionospheric studies the solar cycle has to be considered based on sunspot numbers and 2013 may well be considered as maximum period.

a) Thanks for your observation. The year 2013 was considered as a MSA year based on the description of the solar flux intervals as specified by past studies including Abdu et al.,2003; Wang et al., 2017. Furthermore, the vertical plasma drift is the major controlling parameter in the study of ESF occurrence and the solar flux dependence of this parameter is well understood (Abdu et al., 2010; Oyekola et al., 2007). Thus, the focus is mainly the seasonal variation of the ESF pattern across the considered solar flux interval. We will also like to refer to recent studies (Aswathy et al., 2018; Li et al., 2016) where year 2013 was described as MSA in a similar analysis of ESF occurrence.

2. Equation 1 is confusing and probably wrongly typed. Proper explanation on how Figures 4 and 5 are calculated has to be given. I wonder why the authors cannot simply take ‘(no. of 15 (or 10) min points with RSF/total no. of 15 (or 10) min points for that local time)x100’ to get the occurrence percentage.

a) We have deleted the statement which might have caused the confusion about the considered interval. Hence, the highlighted statements have been changed to;

"Since the ESF events are very rare during the daytime, our investigation was limited to the time interval between 18:00 – 06:00 LT. The ionograms were examined at an hour interval for the presence of range spread F (RSF) or strong range spread F (SSF). Subsequently, the monthly mean of the RSF occurrence percentage variation over the defined local time interval was then estimated using the relation:

$$hourly\ occurrence\ \% = \frac{number\ of\ ionograms\ in\ each\ hour\ with\ RSF}{total\ number\ of\ ionograms\ in\ an\ hour\ for\ that\ month} \times 100 \quad (1)\text{"}$$

3. For March equinox, why the authors select April instead of March. Isn't it more appropriate if they select March, June, September and December? Anyhow, I believe the results may not vary considerably between March and April. They may cross check and explain.

a) Thanks for your observation. We have compared the occurrence rate during the equinoctial months of March and September with the presented results. We found out that the occurrence rate does not vary significantly at these longitudes as you have assumed except during March at the Brazilian station. Where an occurrence percentage of ~70% (88.9%) was observed instead of the ~35% (~70%) recorded during April of the LSA (MSA). However, a similar equinoctial asymmetry pattern is still highlighted in this region during but the difference observed during the MSA will mean the asymmetry peak will occur at M-equinox. We will make the relevant changes to the FZA station.

4. Line 184 – 186. Ilorin data is unavailable during MSA. So this sentence is not appropriate and there may be variations in local time of occurrences over Ilorin between MSA and LSA.

a) Though, the observed large RSF occurrence during LSA means a 50% increase can not be recorded during MSA as stated but we believe the statement is actually unnecessary and it has been deleted.

5. Line 187 – 188. But from Figure 4, during LSA, September was higher than March over Fortaleza, and also at Kwajalein.

a) Thanks for the observation, the statement has been rewritten as;

"Unlike the inconsistent longitudinal variation of the equinox asymmetry pattern observed during the LSA period, the M-equinox has a significantly higher RSF occurrence percentage at the CPN, JIC and KWJ stations"

6. Figure 7. Check panels a and b. Are they interchanged? As per statistics Ilorin do not have data during MSA but as per this plot, it does not have during LSA.

a) Thanks. We will make the necessary correction to the figure caption (Figure 7b should represent the LSA).

7. Line 291 – 296. Not acceptable based on result. Figure 7 shows that there is no PRE over Kwajalein except for S-equinox of MSA. How it can be an example for control of PRE?

a) Thanks for your suggestion. This section has been reviewed and edited to give an improved analysis of our observation.

8. Line 296 – 301. The authors explain based on results of Su et al., (2009). However, with Figure 7 the effect of PRE and associated PSSR can be directly compared and studied. Instead of such an approach

why the authors explain the previously reported results herein? May be previous observations can be moved to the introduction.

a) This section have been edited based on your suggestion.

9. Figure 8. Is the dip equator for Ilorin correct in this Figure?

a) Thanks for your observation, the error was made while converting geographic lat. to geomagnetic lat. using the wdc model (http://wdc.kugi.kyoto-u.ac.jp/cgi-bin/kp-cgi). We have changed it to the quasi-dipole latitude (deg).

10. The text sizes in the Figure labels are small. Enlarge them so that they will be easy to read.

a) Thanks for the observation, this will be corrected

Minor comments:

11. Line 18. The authors mention 2009 or 2010 and 2011 or 2013. What do they mean? Is it like ‘2009 to 2010’ or ‘2009 and 2010’?

a) This have been corrected. The data taken during Oct, 2009 (72.14 sfu) was only used to represent the RSF occurrence at this region during the LSA period due to the low data availability during Oct, 2010 (81 sfu) at the Jicamarca station. We assumed that there will be negligible difference between the background ionospheric condition and subsequently the ionospheric parameters driving the spread F initiation at this region during both years. The highlighted statement will be deleted and the specific season and station where data was taken in the year 2009 will be indicated during the manuscript review.

12. For all the locations, include quasi-dip latitudes also.

a) Thanks for your suggestion. This will be added

13. Lines 47 – 50. While PRE is an important parameter for spread F occurrence, recent works indicate that lack of PRE do not preclude formation of spread F. Spread F forms without PRE as well. This need to be discussed and the identification of late night spread F in many of the previous works have to be cited. Some relavent references are Sastri, Ann. Geophys., 1999; Stoneback et al., JGR, 2011; Candido et al., JGR, 2011; Narayanan et al., EPS, 2014.

a) Thanks for your suggestion. We have included the following sentences;

“Though, recent studies (Candido et al., 2011; Narayanan et al., 2014; Stoneback et al., 2011) have also analyzed the probable role of several other parameters involved in the plasma irregularity initiation over the period characterized by weak background ionospheric condition. Observation of large ESF occurrence rate during the low solar activity have been attributed to the modulation of the post-sunset electrodynamics by the gravity wave induced perturbation electric field (Abdu et al., 2009; Aveiro et al., 2009). While the neutral wind intensity and direction is a dominant factor in the observed post-midnight ESF occurrence pattern (Dao et al., 2017; Sastri et al., 1994).”

14. Line 53 – 55. Distortion of HF signal quality does not affect GPS frequencies. During spread F times, quite often the L band signals themselves get affected. Rewrite accordingly.

a) This has been changed to “…*often distort the L-band signal, thereby causing*…”.

15. Lines 57, 58, 417. Singular to plural: ‘ionopsheric conditions’, ‘deliberate efforts’, ‘charged particles’.

a) The suggested changes have been made accordingly

16. Lines 75 – 77. Initiation depends on seeding also. Though authors are aware of it as discussed in later part of the paper, this statement needs to be rewritten.

a) Thanks, this has been corrected.

"Hence, the large vertical drift enhances the plasma instability triggered by the seed perturbation and subsequently the R-T instability growth rate."

17. Line 82. The references here are not complete. The first works where STBA hypothesis had originated are not given. Give Maruyama and Matuura, 1984 and Tsunoda, 1985.

a) Thanks, we have added the suggested references

18. Line 83. Polarization field or PRE field?

a) It has been changed to "PRE"

19. Line 116. Remove initials of Dr. Galkin in the reference.

a) This has been edited

20. Figure 1 caption. What is shown is geographic latitude longitude map, while the captions claim 'geomagnetic location'.

a) Thanks, this has been corrected.

21. Line 208 – 209. '..both stations..'. Which ones? Give the names.

a) The names (JIC and FZA) have been included

22. Line 214 – 215. But Figure 6(b) shows differences between MSA and LSA in S-equinox and D-solstice period. Particularly during S-equinox. Justify or modify the statement.

a) This statement have been deleted and the preceding statement edited as;

"The observed inverse solar flux dependence pattern at the Brazilian longitude during the S-equinox could be an effect of the solar flux dependence of the density scale length on the RSF occurrence percentage during this season. While, the S-equinox and D-solstice seasons are considered to have a very conducive ionospheric conditions for the generation of ESF at this longitude region during LSA."

23. Give expansion of PSSR in first place of occurrence.

a) Thanks for the observation

24. Line 229. '..the generation of post-midnight ESF events'.

a) Thanks, "*generation of*" have been added to the sentence.

25. In Figure captions either give full station names or give abbreviations, consistently.

a) This has been corrected to full station names

26. Line 252 – 255. How zonal wind affect the vertical plasma drift? Explain briefly.

a) Thanks for the correction, the "*zonal wind*" has been deleted from the sentence.

27. The explanation of terms L and gamma are missing in Equation 2.

a) The equation has been deleted based on the suggestion of Referee 1

28. Line 332 – 334. Give references for the sentence 'post-sunset vertical drift was established to have a directly proportional relationship with the neutral density'.

a) References have been added.

29. Line 363. I disagree. There are indications that ITCZ may influence ESF activity. It is not established yet. More research is required in this regard.

a) We sincerely appreciate your observation with regards to our analysis on the probable influence of ITCZ on the seasonal distribution of ESF activities. We have attempted to demonstrate the complementary role of the gravity wave (GW) in the solstitial asymmetry observed at the low declination angle region using OLR measurement as a proxy for the seasonal distribution of the GW activities at each region. We assume your reservation about this approach might be connected with the results from Su et al., (2014). However, a recent study have attributed the poor correlation at some of the regions with the averaging of OLR value over a wide longitude range (Li et al.,2016). Furthermore, our result showed that the suggested approach does not increase the correlation coefficient at CPN. Hence, we have presented a brief the major factors that could have contributed to the small ESF occurrence percentage at the CPN longitude in spite of the large OLR frequency.

We agree with the opinion that more study is required to fully establish the relationship between the occurrence of OLR measurement and the observed RSF, while we hope the suggested perspective in this paper contributes to related discussion.

30. Line 368. Briefly explain GWBA hypothesis herein. In the course of discussion the authors mention it, but some rearrangement is needed to make the flow of paper proper.

a) This section has been re-arranged and some part moved to the result section as suggested by referee 1.

31. Figure 8. Explanation of how the plot is made have to be given. How many years of OLR data are used?

a) Thanks and we have added more relevant information to the description of the plotted data.

32. Lines 436 – 443. The description is confusing. May consider rewriting more clearly.

a) This section have been rewritten as suggested

"The zonal variation of PRE is relatively small across the longitudinal range 90^{o}E – 120^{o}E and 160^{o}E – 240^{o}E, which encloses the CPN and KWJ stations respectively. The weak PRE at CPN results from the large magnetic field strength and a small field line integrated conductivities at this longitude sector. While, the zonal E field was shown to have the minimum value at the KWJ longitude region and consequently the generally weak PSSR observed at these regions during the LSA (Figure 7b.). Under such circumstance, the GW induced perturbation electric field might have negligible impact on the instability growth across these longitudes in spite of the large OLR frequency. Hence, the negative correlation observed between the OLR frequency and the RSF occurrence percentage at both sectors is associated with the unfavourable background ionospheric condition for the plasma irregularity growth."

~~S~~Observation of the seasonal asymmetry in the Range spread F occurrence ~~features~~ at different longitudinal regions during low and moderate solar activity

Abimbola O Afolayan[1], Singh J Mandeep[1,2]*, Mardina Abdullah[1,2], Suhaila M Buhari[2,3] , Tatsuhiro Yokoyama[4], Pornchai Supnithi[5]

[1] Center of Advanced Electronic and Communication Engineering, Universiti Kebangsaan Malaysia, 43600 Bangi, Selangor, Malaysia.

[2] Space Science Centre (ANGKASA), Institute of Climate Change, Universiti Kebangsaan Malaysia, 43600 Bangi, Selangor, Malaysia.

[3] Geomatic Innovation Research Group, Faculty of Science, Universiti Teknologi Malaysia, 81310 Johor Bahru, Johor, Malaysia.

[4] Research Institute for Sustainable Humanosphere, Kyoto University, Uji, Japan

[5] Faculty of Engineering King Mongkut's Institute of Technology Ladkrabang, Bangkok, Thailand

Correspondence to: Singh J. Mandeep (mandeep@ukm.edu.my)

Abstract

A comparative study of the equatorial spread F occurrence was conducted at different longitudes during ~~2009 or~~ 2010 and ~~2011 or~~ 2013 which represents the low (LSA) and moderate (MSA) solar activity periods respectively. The ionogram data were recorded at low latitude stations including Jicamarca (JIC; 75.76^{o}W, 8.17^{o}S), Peru; Fortaleza (FZA; 38.52^{o}W, 3.73^{o}S), Brazil; Ilorin (ILR; 7.55^{o}E, 9.93^{o}N), Nigeria; Chumphon (CPN; 88.46^{o}E, 11^{o}N), Thailand and Kwajalein (KWA; 167.73^{o}E, 8.72^{o}N), Marshal Island. The range type spread F (RSF) occurrence was manually recorded at an hour interval between 18:00 – 06:00 LT and a monthly average of the RSF occurrence was estimated for each of the seasons. The ~~observed~~ longitudinal distribution ~~features of the~~ of the RSF occurrence features ~~and its longitudinal distribution at different seasons~~ include the observed difference in the onset time, duration and seasonal occurrence peak ~~of occurrence~~. The ~~significant observations include the~~ seasonal asymmetry~~ie~~ in the RSF occurrence distribution ~~during the equinoctial season at most of the longitudes, while during the solstice seasons there are cases of discrepancy in the RSF occurrence with respect to the sunset terminator-magnetic field alignment~~was analyzed in relation with the zonal drift reversal's effect on the plasma irregularity initiation. We believe that the inconsistent equinoctial asymmetry pattern in the RSF occurrence is modulated by the seasonal/longitudinal variation of the zonal drift reversal delay during both solar epochs. Likewise, the seeding effect and the background

ionospheric condition were also considered as the major factors influencing the frequency of irregularity generation at these regions.~~The inconsistent pattern of the RSF occurrence percentage and the post-sunset rise of the F layer in relation to the sunset time lag were analyzed. While the possible role of the seed perturbation effect was discussed with respect to some of the peculiar features observed in the longitudinal/seasonal distribution of the spread F occurrence percentage.~~

Keywords: Equatorial Spread F; Vertical plasma drift; R-T instability; ~~OLR~~zonal drift, EEJ.

1. Introduction

The equatorial spread F (ESF) is a nighttime phenomenon that describes the observed ionospheric F layer electron density irregularity within the equatorial or low latitude region and it is usually depicted as the wide spread of the echo trace on the ionogram measurement (Booker and Wells, 1938; Bowman, 1990). This echo spread along the frequency band or height range is due to the scattered signal reflection from the multiple paths caused by the irregular ionospheric plasma density profile. The scale size of these plasma irregularities ranges between a few centimeters and hundreds of kilometer (Basu et al., 1978; De Paula et al., 2010). The ESF is usually initiated after the local sunset due to the rapid rise of the F layer and this generates a steep bottom-side plasma density gradient as a result of the abrupt reduction of the E region ionization level. The Raleigh-Taylor (R-T) instability excited in the bottom-side is considered as the mechanism responsible for the initiation and non-linear growth of the plasma depletion (Woodman and La Hoz, 1976). The vertical plasma drift near the local post-sunset driven by the pre-reversal enhancement (PRE) of the zonal electric field ~~vertical drift velocity responsible for the uplift of the F layer in conjunction with the R-T instability mechanism~~ is recognized as the ~~basic drivers~~ major factor controlling the ESF morphology across the different seasons and longitudes (Abdu, 2001; Dabas et al., 2003; Lee et al., 2005). The PRE rapidly elevates the ionosphere into a higher altitude region, where the collision frequency is lower and more conducive for further plasma depletion growth by the R-T instability mechanism (Fejer et al., 1999; Woodman and La Hoz, 1976). Though, recent studies (Candido et al., 2011; Narayanan et al., 2014; Stoneback et al., 2011) have also analyzed the probable role of several other parameters involved in the plasma irregularity initiation over the period characterized by weak background ionospheric condition. Observation of large ESF occurrence rate during the low solar activity have been attributed to the modulation of the post-sunset electrodynamics by the gravity wave (GW) induced perturbation electric field (Abdu et al., 2009; Aveiro et al., 2009). While the neutral wind intensity and direction is a dominant factor in the observed post-midnight ESF occurrence pattern (Dao et al., 2017; Sastri et al., 1994).

The plasma irregularity occurrence around the equatorial/low latitude region ~~causes~~ often ~~distortion~~ distorts ~~of~~ the L-band ~~HF~~ signal ~~quality~~, thereby ~~inducing~~ causing a poor performance of the communication or navigation systems such as the Global Positioning System (GPS) ~~(Seif et al., 2015)~~. Therefore, it is important to understand the role of the different precursory factors influencing the spread F morphology under varying ionospheric conditions. This complex phenomenon has been explored widely by past studies (Su et al., 2009; Tsunoda, 2010a; Vichare and Richmond, 2005) and there are presently deliberate efforts to improve the prediction accuracy of spread F occurrence distribution pattern across the different regions.

The complex interaction between the E and F region dynamo system in the presence of conductivities and the magnetic field are responsible for the different electrodynamic phenomenon at the low latitude region (Haldoupis et al., 2003; Miller, 1997). During the daytime, the F region divergent current causes an accumulation of the downward polarization electric field at the bottom-side of the region. On the other hand, the E region polarized electric field concurrently drives a closure current mapped along the magnetic field line into the F region that diminishes the F region vertical current (Abdu et al., 1981; Eccles et al., 2015; Heelis, 2004). The field line integrated Pedersen conductivity shorts out the F region dynamo electric field and significantly reduces the zonal plasma drift due to the high E region conductance during the daytime. However, the decay and the consequent reduction of the E region conductance during the nighttime causes a significant increase in the field-aligned Pedersen conductivity ratio. This generates a large vertical current by the F region dynamo and the resulting downward electric field drives the plasma in the direction of the neutral wind. Thus, the F layer dynamo electric field created by the divergence current dominates near the sunset period and this induces the eastward plasma motion in the F region at an ***E*** x ***B*** velocity. The PRE vertical plasma drift is associated with the enhanced eastward electric field caused by the significant decay of the E region conductivity.

This combined with the rapid chemical recombination rate of the E layer around the sunset period results in the increased steepness of the bottom-side plasma density gradient. Hence, the large vertical drift enhances the plasma instability triggered by the seed perturbation and subsequently the ~~initialization of the~~ R-T instability growth rate. On the other hand, a prolonged eastward equatorial electrojet (EEJ) could cause a reduced field aligned conductivity gradient due to the small vertical current driven by the post-sunset conjugate E region. Thus, the resulting zonal electric field accumulation at the F layer base can only generates a relatively small PRE vertical drift. This ionospheric electrodynamics effect also yield a zonal drift reversal delay which have also been shown as a strong factor influencing the instability growth rate (Su et al., 2009).

The seasonal/longitudinal distribution of the ESF occurrence rate is dependent on the declination angle of the magnetic field. The longitudinal gradient of the field-aligned Pedersen conductivity becomes steepest when the sunset terminator is well aligned with the local magnetic flux tube, thereby resulting in a simultaneous relative sunset time at the magnetic conjugate E regions that are coupled to the F region (Abdu et al., 1992; Maruyama and Matuura, 1984; Tsunoda, 1985; Tsunoda et al., 2015). Hence, the PRE of the eastward ~~polarization~~ electric field is maximum at such longitude and likewise the elevation of the F layer altitude near sunset. The base of the F region gets lifted to greater heights making it conducive for the plasma instability growth. Therefore, the longitudinal variation in the seasonal distribution of the ESF occurrence rate is associated with the variation of the solar terminator-magnetic field alignment (STBA) and their distinct local sunset time equatorial electric field system. Due to the near-zero sunset time lag between the conjugate E regions during the equinox period, there is usually a good alignment. On the other hand, the solstice months have been shown in several studies (Hoang et al., 2010; Su et al., 2008) to have good (bad) alignments during June solstice (December solstice) at longitudes of positive (negative) magnetic declination. The seasonal/longitudinal distribution of the equatorial plasma irregularity has been extensively reported to be strongly correlated with the seasonal variation of the STBA (Abdu et al., 1981; Li et al., 2008; Su et al., 2008). However, a recent study described the significant ESF occurrence during the solstice seasons at the West African and Central Pacific region to be inconsistent with the defined theory of the declination angle influence on the spread F longitudinal distribution (Tsunoda et al., 2015). Likewise, Huang, (2017) reported an anti-correlation between the vertical plasma drift and the small amplitude irregularity during the moderate solar activity period. These discrepancies are considered noteworthy for an improved understanding of the features of global plasma irregularity distribution as influenced by different background atmospheric conditions~~s~~.

The main focus of this study is to examine the salient features of the spread F local time distribution patterns at these longitude sectors during the equinox and solstice~~different~~ seasons of the low (2010: 80sfu) and moderate (2013: 122.7sfu) solar activity period~~at the different longitude sectors~~. Furthermore, the role of the zonal drift reversal time was investigated in relation to the observed asymmetry during the equinox and solstice seasons. Though the asymmetry pattern during the equinoxes is yet to be well defined and it varies across the longitudes during both solar epochs. This analysis tended to understand the major phenomenon responsible for the equinoctial asymmetry of the ESF occurrence at each region. Thus, the ~~possible~~ probable competing role of the vertical plasma drift, virtual height and the seed perturbation were considered in the analysis of the observed spread F distribution at these ~~for the considered~~ longitude sectors~~will be discussed~~.

2. Data and methods

The ESF events were recorded at the equatorial stations situated at different longitudes (Jicamarca (JIC) station, Peru; Fortaleza (FZA) station, Brazil; Ilorin (ILR) station, Nigeria; Chumphon (CPN) station, Thailand and Kwajalein (KWJ) station, Marshal Island), as shown in Table 1. The table lists the geographic coordinates and the sunset time at each of the stations selected for the study of the spread F irregularity distribution. These are stations within the Southeast Asia low-latitude ionospheric network (SEALION) and Global Ionospheric Radio Observatory (GIRO) network as indicated in Fig.~~ure~~ 1. The observation data were taken using the digital ionosonde (DP-S 4 digisonde) and analogue type FMCW (frequency modulated continuous wave) (Maruyama et al., 2008; Reinisch and ~~I. A.~~ Galkin, 2011). Since the ESF events are very rare during the daytime, our investigation ~~is~~ was limited to the time interval between 18:00 – 06:00 LT. ~~Though the ionograms were recorded at different intervals at each~~

~~of the stations, we analyzed the ionogram at 15 min interval during the nighttime hours, except that of the Fortaleza station which was set at 10 min interval. Each~~ The ionograms ~~is~~ were examined at an hour interval for the presence of range spread F (RSF) or strong range spread F (SSF) ~~according to the defined interval~~. Subsequently, the ~~hourly~~ monthly mean ~~variation~~ of the RSF occurrence percentage variation over the defined local time interval was then estimated using the relation:

$$hourly\ occurrence\ \% = \frac{number\ of\ ionograms\ in\ each\ hour\ with\ \cancel{E}RSF\ \cancel{in\ the\ hour}}{total\ number\ of\ ionograms\ in\ an\ hour\ \cancel{over}\ for\ th\cancel{at}e\ month} \times 100 \qquad (1)$$

Only the quiet days ($\Sigma k_p \leq 24$) were considered for each month representing the different seasons during the low (F107A < 100 sfu) and moderate (F107A < 150 sfu) solar activity period (Wang et al., 2017). The seasonal variation of the ESF events ~~across the different longitudes~~ was analyzed according to the available data at each of the ionosonde stations listed in Table 1. Thus, the data taken from ~~April~~March, June, September and December months of 2010 (2013) represents the March equinox, June solstice, September equinox and December solstice of LSA (MSA) respectively.

Table 1: Description of the stations' geographic location and their local sunset time range.

Station	Longitude (degree)	Latitude (degree)	Dip Latitude	Declination angle	Sunset time (LT)
Jicamarca (JIC)	-75.76	-8.17	3.75	-3.24	18:45 – 19:15
Fortaleza (FZA)	-38.52	-3.73	-6.89	-20.11	18:30 – 18:45
Ilorin (ILR)	4.5	8.53	-4.27	-1.69	18:00 – 19:00
Chumphon (CPN)	99.37	11	3.76	-1.46	19:30 – 20:15
Kwajalein (KWJ)	167.73	8.72	3.62	7.62	19:30 – 20:15

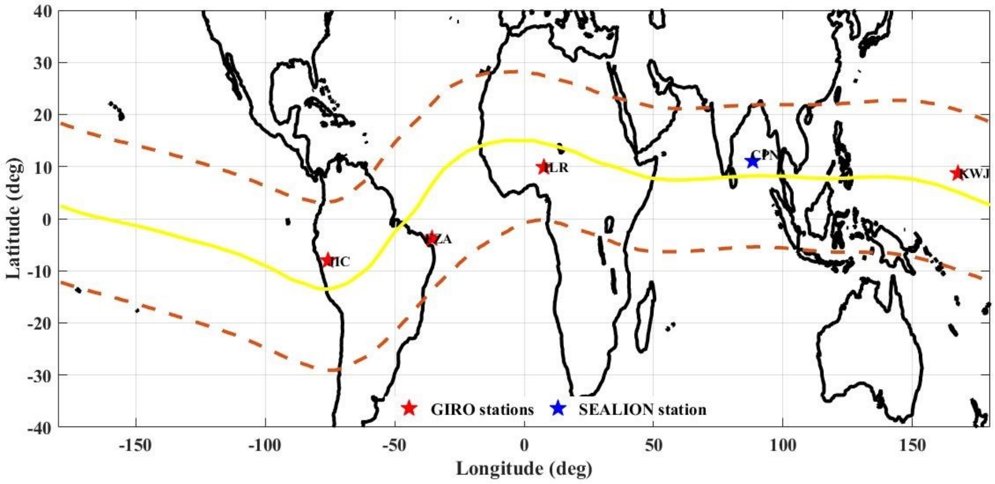

Figure 1: The ~~geomagnetic~~ geographic location of the ionosonde stations and their corresponding observatory network shown by the red (GIRO) or blue (SEALION) marker.

The recorded ionogram ~~echo spread~~ signatures are usually divided into frequency spread F (FSF), mixed spread F (MSF), range spread F (RSF) and strong range spread F (SSF) (Shi et al., 2011). However, this study considers only the RSF and SSF type during the manual observation of the plasma irregularities across these longitudes. The RSF signature represents the instance of the main F layer trace ~~echo~~ spreading mainly along the ~~height axis~~altitude as shown in Figure 2, ~~while~~ and the SSF which is described as a type of RSF has its ~~with the F layer~~ main trace ~~echo significantly~~ extending significantly beyond the local foF2 (Bowman, G. G., 1960; Bowman, 1998). Hereafter, we will refer to ~~both types of spread F as RSF, while~~ the March, June, September and December seasons ~~regarded~~ as M-equinox, J-solstice, S-equinox and D-solstice respectively.

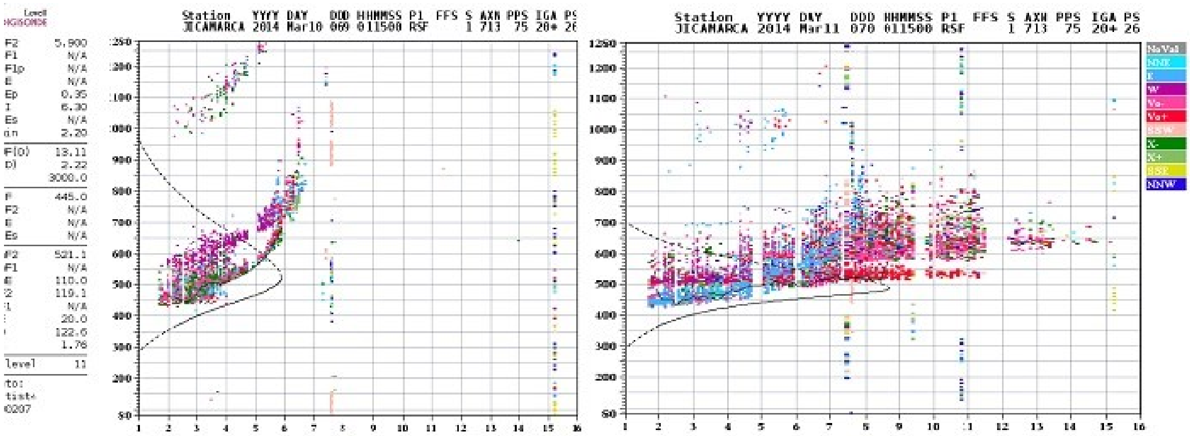

Figure 2: Sample of the RSF (left) and SSF (right) recorded using the DPS-4 digisonde at the Jicamarca station.

The monthly average of the scaled virtual height was taken as a representation of the seasonal variation of the near sunset vertical plasma drift recorded at each of the ionosonde stations. The seasonal variation of the virtual height taken during the low solar activity (LSA) and moderate solar activity (MSA) period was then analyzed in correspondence to the RSF occurrence distribution. Based on data availability across the considered stations as shown in Figure 3, the data taken during the year of ~~2009 or~~ 2010 represents the LSA period while the year of ~~2011 or~~ 2013 ~~is taken for~~represents the MSA period. ~~Since the solar flux unit is similar, we consider it acceptable to make a comparison between the RSF occurrence pattern during the mentioned years for the LSA and MSA period.~~

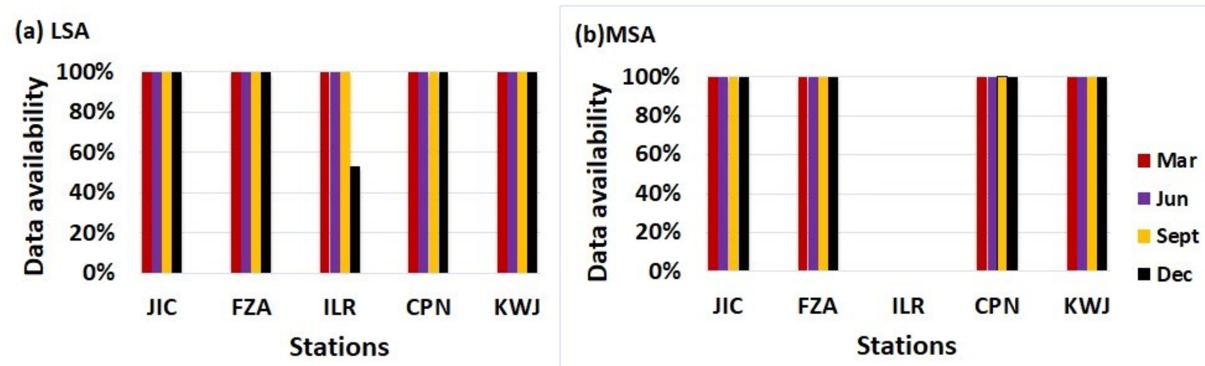

Figure 3: The ionogram data availability at the Jicamarca, Fortaleza, Ilorin, Chumphon and Kwajalein stations during the (a) LSA and (b) MSA period.

3. Results

Figures 4 and 5 present the ~~nighttime~~ hourly ~~variation~~ distribution of the ~~monthly mean of the~~ RSF occurrence percentage across the different longitudes during the LSA period and the MSA period, which were averaged over each month based on the available data at these ~~different~~ stations. ~~The seasonal variation of the RSF occurrence pattern across the different longitude regions was represented as a histogram of the spread F occurrence rate during the LSA and MSA period. Generally, the average duration of the post-sunset plasma irregularity in Figure 4 varies across the longitude, while the start time of the spread F varies mostly between 18:00 and 20:00 LT during the equinox and D-solstice months. The observed variation in the start time of the RSF occurrence corresponds with the varying sunset time across the different longitudes as shown in Table 1.~~ The monthly ~~average of the~~mean RSF occurrence percentage ~~is~~ was higher at all the considered longitudes during the equinox months than the solstice months of the LSA year. The percentage of RSF occurrence percentage and duration is highest at the ILR station for all the seasons, while the ~~average lowest~~ minimum monthly mean RSF occurrence percentage was recorded at the ~~CPN~~ KWJ station. Generally, the average duration of the post-sunset plasma irregularity in Fig. 4. varies across these longitude sectors, while the starting time of the spread F during the equinox and D-solstice months varies mostly between 18:00 and 20:00 LT. The observed onset time variation of the RSF occurrence corresponds with the varying sunset time across the different longitudes as shown in Table 1, except cases with significant delay. ~~Li et al., (2011) showed that most post-midnight plasma irregularity occurrence in the African region were initiated during the post-sunset period.~~Figure 4 shows that the maximum RSF occurrence percentage was mostly observed before the midnight period (around 21:00 LT) during most seasons at each longitude. However, there are months which have a significantly larger RSF occurrence percentage near the midnight than at 21:00 LT. This could be attributed to either the irregularity onset delayed till pre-midnight period as a result of the ionospheric condition or multiple days with irregularities drifting from distant location into the ionogram's field of view (Balan et al., 2018; Narayanan et al., 2014). ~~It is also~~

Another important ~~to highlight~~observation was the ~~significantly high~~ large ~~probability of~~ RSF occurrence percentage of ~70 % at ~~the~~ ILR ~~and~~ but relatively smaller occurrence rate of ~30 % at KWJ ~~stations~~ during the J-solstice ~~month~~ of the LSA year. ~~Unlike~~ While ~~the other longitude regions where~~ the RSF occurrence percentage ~~i~~was below 10% at the other longitude regions~~during this period~~. The large RSF occurrence percentage recorded at the ILR stations was contrary to the expected longitudinal distribution based on the defined low and high ESF longitude range during the J-solstice (Su et al., 2007). ~~Furthermore, the plasma irregularity onset time during the M-equinox and J-solstice at the KWJ station was delayed by ~2hrs after the local sunset time.~~ Likewise, the other relevant observations across the different longitudes during the J-solstice, such as the significantly delayed irregularity onset at KWJ will be further discussed in a later section.

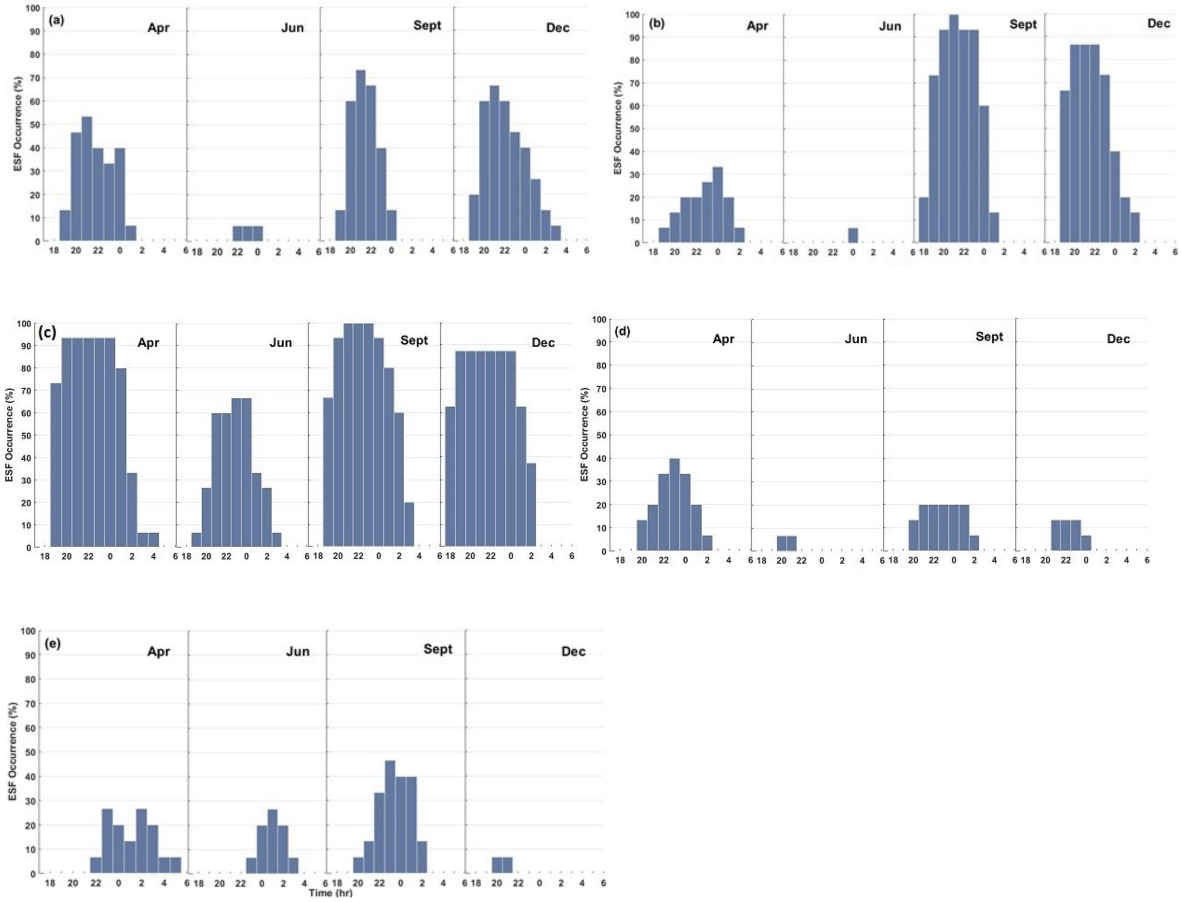

Figure 4: Occurrence rate of RSF during LSA period at the (a) Jicamarca (b) Fortaleza (c) Ilorin (d) Chumphon and (e) Kwajalein stations.

Figure 5~~,~~ shows that there was ~~more than~~above ~~5~~30% increase in the RSF occurrence percentage across all the stations during the M-equinox ~~months~~ of the MSA period ~~across all the stations~~. ~~except at the ILR station, where ~100 % was already recorded during the LSA.~~ The spread F equinox asymmetry was very visible in all the regions except at the FZA station~~,~~, where ~~T~~the hourly peak of the RSF occurrence percentage ~~hourly peak~~ was approximately ~~the same~~equal at both equinox seasons. ~~at the FZA station~~. Unlike the equinoctial~~x~~ asymmetry ~~pattern, observed~~ during the LSA which showed an inconsistent longitudinal variation ~~period,~~ the M-equinox has a significantly ~~high~~larger RSF occurrence percentage at the CPN, JIC and KWJ stations during the MSA. On the other hand, Fig.~~ures~~ 4 and 5~~,~~ show ~~the~~ a similar~~ity~~ solstice asymmetry ~~between~~ in the observed RSF occurrence percentage ~~-~~during ~~the solstice months of~~ both solar epochs. The RSF occurrence percentage during the J-solstice of the MSA period was less~~er~~ than or ~10 % at all the stations except at the KWJ station. ~~Likewise, t~~There was ~30 % increase in the ~~recorded~~ RSF occurrence percentage at the KWJ station during J-solstice and the irregularity onset time was also much earlier (immediately after the local sunset) than the LSA onset time. ~~(~~Su et al., (2009) have already established a relationship between the zonal drift reversal time and the velocity drift amplitude, instability growth rate and irregularity onset in the 150^0 - 170^0 longitude range. Hence, the delayed onset and the relatively small RSF occurrence percentage at this region during the LSA will later be discussed further in relation to the zonal drift reversal effect and the weak background ionospheric condition in the region.

~~The pre-midnight RSF occurrence percentage peak recorded ~15% increase at the FZA and CPN stations during the D-solstice, while there was no occurrence of RSF at the KWJ station.~~ The ~~largest STBA is observed at the~~ negative declination angle region was described as the high ESF longitude during the D-solstice due to the strong magnetic flux tube-solar terminator alignment (Tsunoda, 1985).~~,~~ Furthermore, the large declination angle in the Brazilian region causes a relatively simultaneous local sunset at the conjugate E region and thereby driving a stronger eastward polarization electric field at the equatorial F region (Abdu et al., 1981; Tsunoda, 2010a). ~~c~~Correspondingly the highest RSF occurrence percentage peak was recorded at the FZA station for both the LSA (~85%) and MSA (~100%) ~~-~~period. The pre-midnight RSF occurrence percentage peak recorded ~15% increase at the FZA and CPN stations during the D-solstice, while there was no RSF occurrence ~~of RSF~~ at the KWJ station during the MSA period. The reduced RSF occurrence percentage at KWJ during D-solstice correlates with the described anti-solar spread F occurrence pattern at the low ESF longitudes during the solstices (Su et al., 2007).

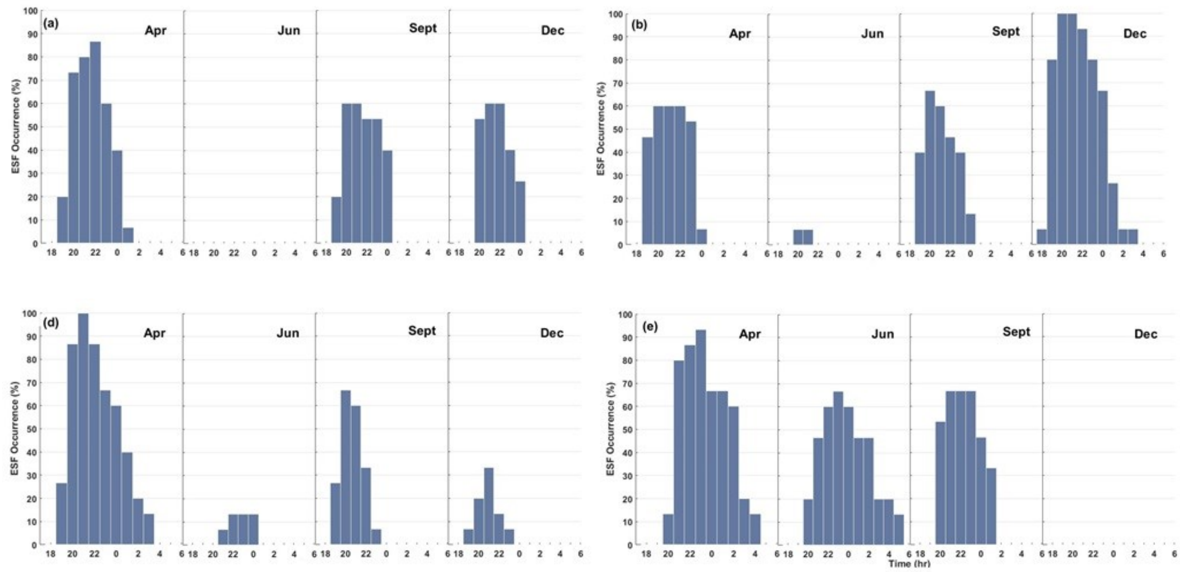

Figure 5: Occurrence rate of RSF during the MSA period at the (a) Jicamarca (b) Fortaleza (d) Chumphon and (e) Kwajalein stations.

Figures 6(a-d) show~~s~~ a comparison ~~of~~ between the ~~ESF~~ RSF occurrence percentage~~s~~ during the MSA and LSA at each of the four stations with sufficient data. There was a significant difference between the spread F occurrence percentage during the LSA and MSA period across all seasons at most of the stations except at the JIC and FZA stations. The ~~ESF~~ RSF occurrence percentage at both stations ~~were~~ varies inversely ~~related to~~with the solar flux index during S-equinox, while ~~and~~ approximately ~~the same~~equal percentage was recorded during the D-solstice of both solar epochs. The observed negative solar flux dependence pattern ~~in the occurrence rate~~ at these ~~Brazilian~~ longitudes during the S-equinox ~~might~~ could be attributed to the ~~fact that the~~growing effect of the density scale length on the ~~average ESF occurrence percentage~~ irregularity growth ~~in this region~~ during this season as the solar flux increases~~is typically high (Su et al., 2007)~~. ~~Furthermore~~Hence, the S-equinox and D-solstice seasons ~~offer~~ were described as having a more conducive ionospheric~~the most favourable~~ condition~~s~~ for the generation of ~~ESF~~ RSF at this longitude region during LSA. ~~Hence, the ESF occurrence percentage as observed in Figure 6(b) is independent of the solar activity index during the S-equinox and D-solstice period.~~

There was ~~non-~~absence of RSF occurrence ~~of RSF~~ at the JIC station during J-solstice of the MSA. ~~presents a similar pattern as the earlier recorded decrease in the plasma irregularity occurrence~~

~~percentage with respect to an increasing solar flux index in this longitude region (Li et al., 2011). Such anti-solar activity alignment of~~The inverse correlation between the solar flux intensity and the RSF occurrence ~~during the solstice seasons~~ have been ~~discussed~~ observed at the low ESF longitudes from 230^0 to 10^0 and 90^0 to 260^0 during the J-solstice and D-solstice respectively~~by~~ (Su et al., 2007)~~Su et al., (2007)~~ and attributed to the neutral wind effect. Their result was corroborated by the diverging neutral meridional wind pattern observed during the J-solstice ~~in~~ at this longitude and the expected effect ~~influence~~ of the increased meridional wind on the irregularity growth suppression during the MSA. The peak ~~E~~RSF occurrence percentage at most of the longitudes during the LSA is usually around the midnight period while ~~in the case of the MSA,~~ the peak is closer to the local sunset time during MSA. However, thorough ~~consider~~observation of the ~~observed E~~RSF occurrence features ~~during LSA~~ as shown in Fig.~~ures~~ 6(a-b) indicated that the near sunset peak and the rapid increase of the RSF occurrence percentage were more consistent ~~with~~ for the seasons ~~having~~ with an expectedly significant post-sunset rise (PSSR)~~ rather than the solar flux index~~. The typical plasma irregularities formed around the sunset period are dominated by the PRE dynamics, while some other mechanisms may play a substantial role in the generation of the post-midnight ESF events (Dao et al., 2017; Otsuka, 2018).

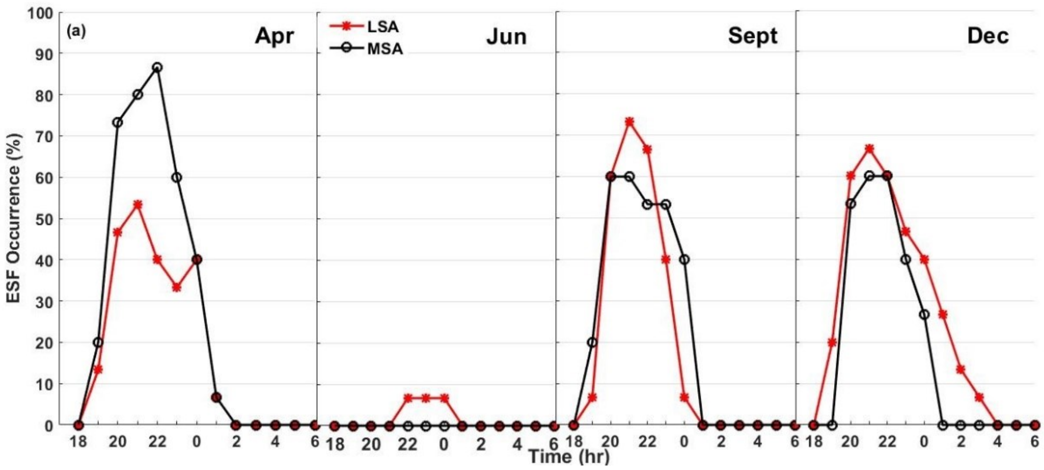

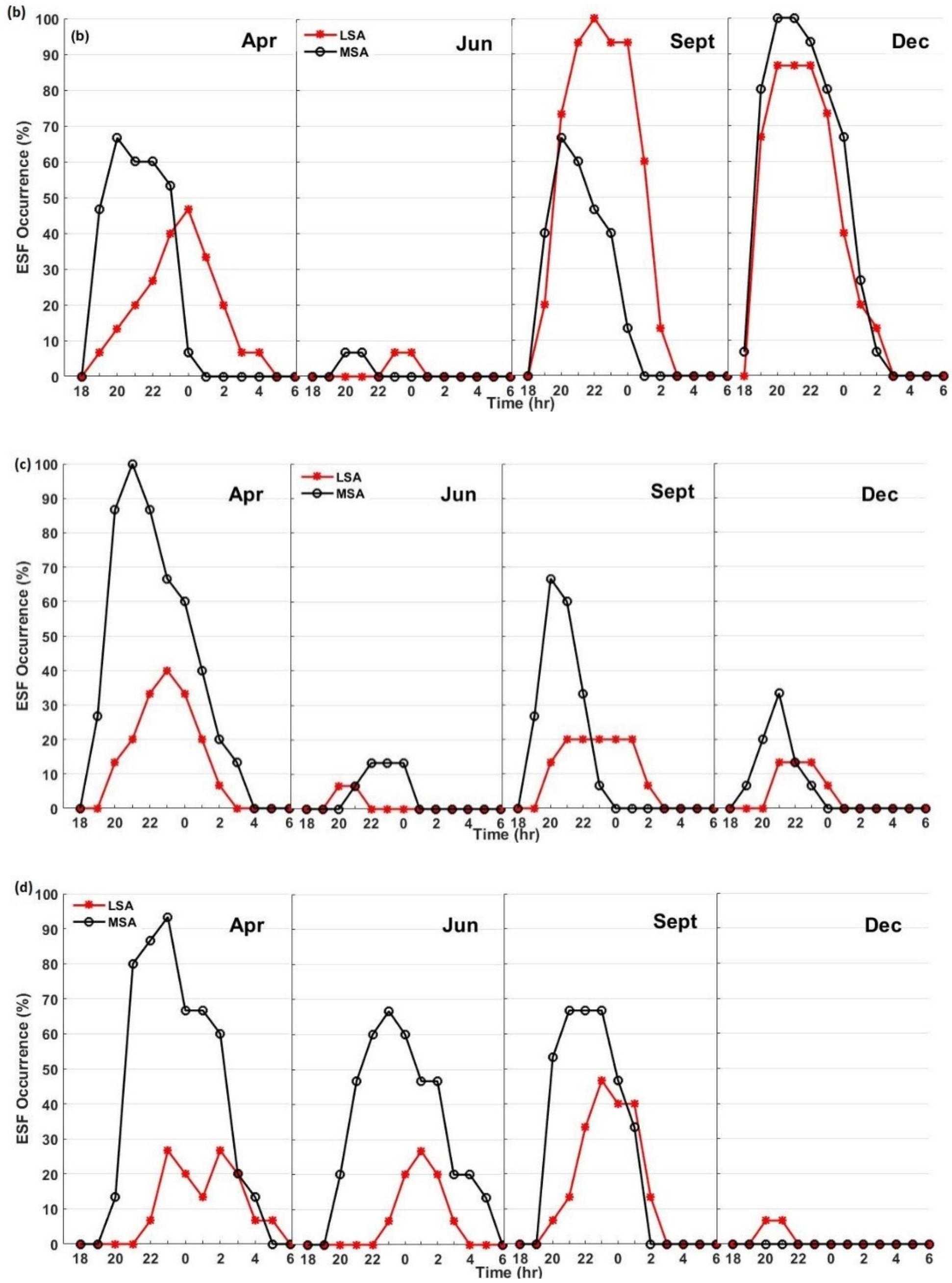

Figure 6: The percentage of ESF occurrence during the LSA and MSA period for (a) ~~JIC~~ Jicamarca (b) ~~FZA~~Fortaleza (c) Chumphon~~CPN~~ and (d) Kwajalein~~KWJ~~ stations.

Figures 7(a-b)~~ & (b).~~ show the local time variation of the monthly mean virtual height (*h'F*) during the LSA and MSA period across the five longitude regions considered in this study. Likewise, the corresponding annual variation of the sunset time lag was also presented in Fig.~~ure~~ 7(c). This represents the difference between the local sunset times at the foot-points of the conjugate E region that connects with the F layer base. The longitudinal variation pattern of the PSSR is consistent with the earlier numerical simulation by Vichare and Richmond, (2005), which observed that the longitudinal PRE variation have its peak between 290^o E and 30^o E longitude region. The observed ~~post-sunset rise~~PSSR of the $h'F$ (representing the ~~evening~~ pre-reversal enhancement (PRE) of the vertical plasma drift near the local sunset) is generally higher during the equinoctial and D-solstice months of MSA than the corresponding seasons of the LSA period. In the case of J-solstice months, the near sunset enhancement of the vertical plasma drift as shown in Figure 7(a-b) was almost absent during both ~~LSA and MSA period~~solar epochs. Though based on ~~our~~ the comparison with the annual sunset time lag variation for each of the regions as shown in Fig.~~ure~~ 7(c) , the PRE magnitude was expected to be larger at the KWJ station than the other regions. However, the relatively large magnetic field strength in the Asian (CPN) and Central Pacific (KWJ) region ~~is quite large~~ (Su et al., 2009; Vichare and Richmond, 2005)~~ and this was responsible for~~causes the weak PRE mostly observed in this regions during both ~~MSA and LSA period~~solar epochs. Such zonal variation of the ~~different~~ factors including the ~~zonal wind,~~ eastward electric field, field-aligned Pedersen conductivity and magnetic field strength contributes to the resultant zonal variation of the vertical plasma ~~drift~~ amplitude (Abdu, 2016; Vichare and Richmond, 2005)~~ across the longitude sectors~~. ~~Our~~

The ~~comparison of the~~ sunset time lag was inconsistent with the ~~corresponding PSSR of the $h'F$ also highlights an inconsistent pattern in the form of~~ observed solstice asymmetry in the PSSR at the low declination angle regions. ~~Similar asymmetry is also prominent during the equinoctial seasons of the MSA at all the regions except the KWJ station where we earlier recognized the inverse effect of the strong magnetic field intensity on the post-sunset PRE vertical drift.~~ The equatorial electrojet (EEJ) ~~was~~ has been identified as a likely controlling factor in the seasonal variation of the near local sunset PSSR~~, while the monthly modulation in the F region eastward neutral wind velocity was found insufficient to describe the observation~~ (Abdu et al., 1981~~; Tsunoda et al., 2015~~). The effect of the post-sunset EEJ presence ~~effect is as a~~ result ~~o~~from the strong dependence of the PSSR on the longitudinal gradient of the Pedersen conductivity. Hence, a seasonal modulation of the EEJ strength by tidal winds from the lower atmosphere will contribute to the PRE. Apart from slow decay of EEJ due to the prolonged sunset duration between the conjugate E regions, the seasonal ionospheric density variation could also influence the field-aligned current and the changes in the zonal drift reversal. ~~Similarly,~~ Su et al., (2009) highlighted the influence of the prolonged eastward EEJ on the zonal drift reversal during J-solstice,~~.~~ ~~W~~which is expectedly ~~to be~~ accompanied by a weak vertical plasma drift in the F region. On the other hand, an equinoctial asymmetry in the PSSR was also prominent during the MSA at all the regions except the KWJ station, where the weak ***E*/*B*** generally reduces the post-sunset PRE vertical drift. The asymmetry is mainly attributed to the increasing difference between the neutral density components at both equinoxes as the solar flux increases (Manju and Madhav Haridas, 2015).

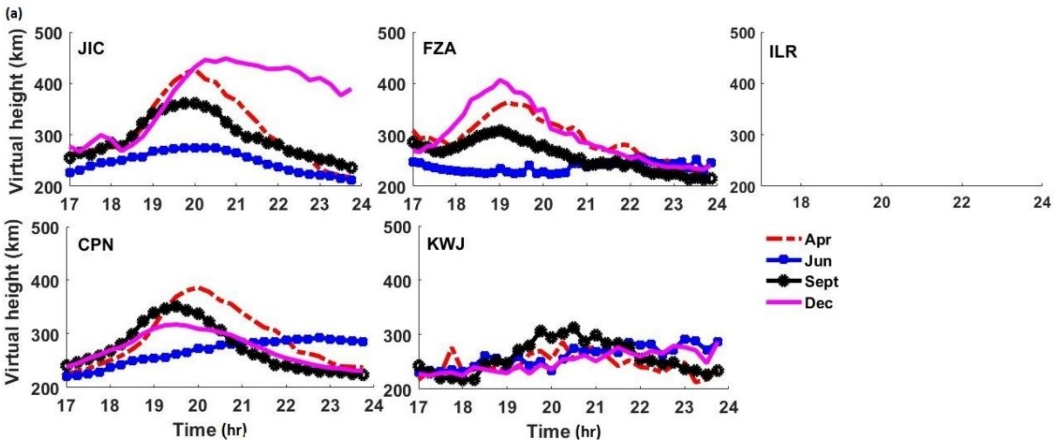

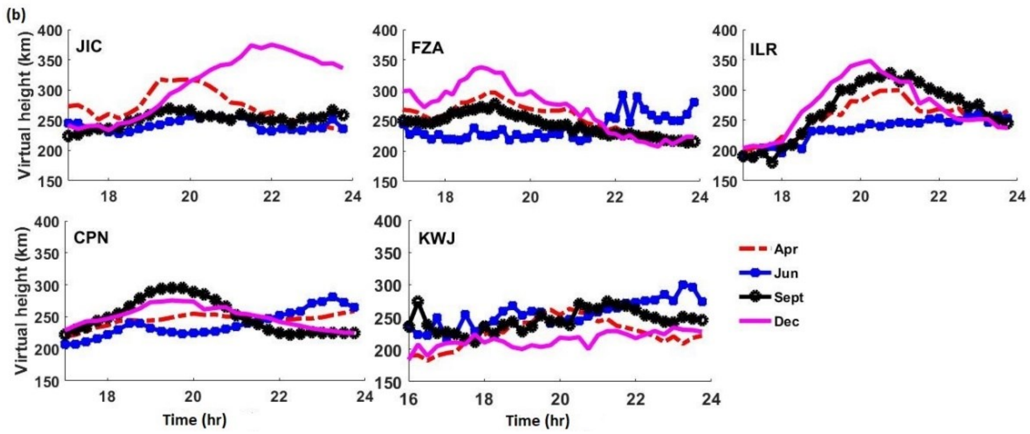

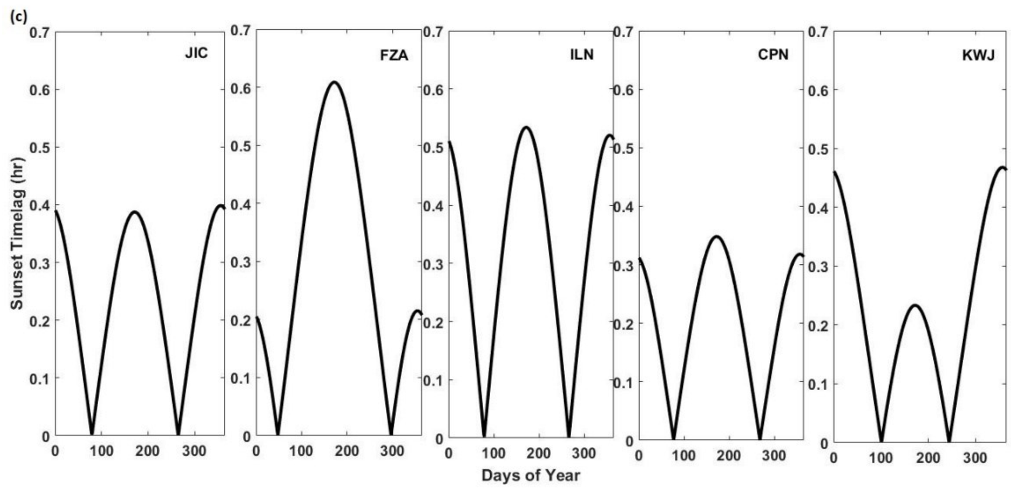

Figure 7: Monthly average of the virtual height during (a) MSA, (b) LSA and (c) The estimated sunset time lag between the geomagnetic conjugate points for each of the longitude sectors.

There has been an extensive discussion on the geometry and coupling of the upward propagating GW considered most suitable for the ESF initiation (Krall et al., 2013a; Tsunoda, 2010b, 2010c). The seeding of plasma irregularity is expected to occur when the phase front of the GW becomes aligned with the magnetic field line ($\vec{B}$). This alignment condition is considered possible, only if the convective active regions are located close to the magnetic dip equator (Tsunoda, 2010a). The geographic map of the OLR measurement provides the longitudinal distribution of the deep convective activity (Gu and Zhang, 2002; Waliser and Gautier, 1993). The seasonal variation of the GW occurrence across the different regions will then be analyzed using the interpolated OLR data that are available from the National Oceanic and Atmospheric Administration NOAA website (http://www.esrl.noaa.gov/psd/data/gridded/data.interp_OLR.html). Which will be compared with the observed seasonal variation of the ESF occurrence percentage across these regions.Figure 8. shows the variation of the monthly averaged OLR distribution across the five stations. The interpolated OLR data taken during 2010 (LSA) by NOAA18 are used. With the measurement taken over 10 degrees longitudinal range which brackets the location of the ionosonde station and ± 20 degrees at both sides of the dip equator (white line). The defined threshold OLR strength used to distinguish regions of convective and non-convective activity was 200 W/m^2 in each bin per day (Gu and Zhang, 2002). The frequency of the OLR occurrences represents the frequency of the GW occurrences in each month. In the JIC and FZA longitude regions ~~where the dip equator is located at the southern hemisphere,~~ we noticed that the GW occurrence peak during the J-solstice is located farther from the dip equator compared to the D-solstice. The observed pattern of the monthly GW distribution displayed a tendency to produce a solstitial asymmetry in the expected seeding effect on the ESF occurrence. On the other hand, an average ~~large~~ OLR occurrence frequency was observed close to the dip equator from January to November at the KWJ longitude. While throughout the year, a varying degree of large OLR occurrence was observed around the dip equator at the ILR and CPN longitudes. A comparison between the OLR occurrence frequency and the RSF occurrence percentage (Figure 4) shows a strong agreement at all the longitudes except the CPN station. Where the observed low RSF occurrence percentage contradicts the large OLR frequency around the dip equator in the region.

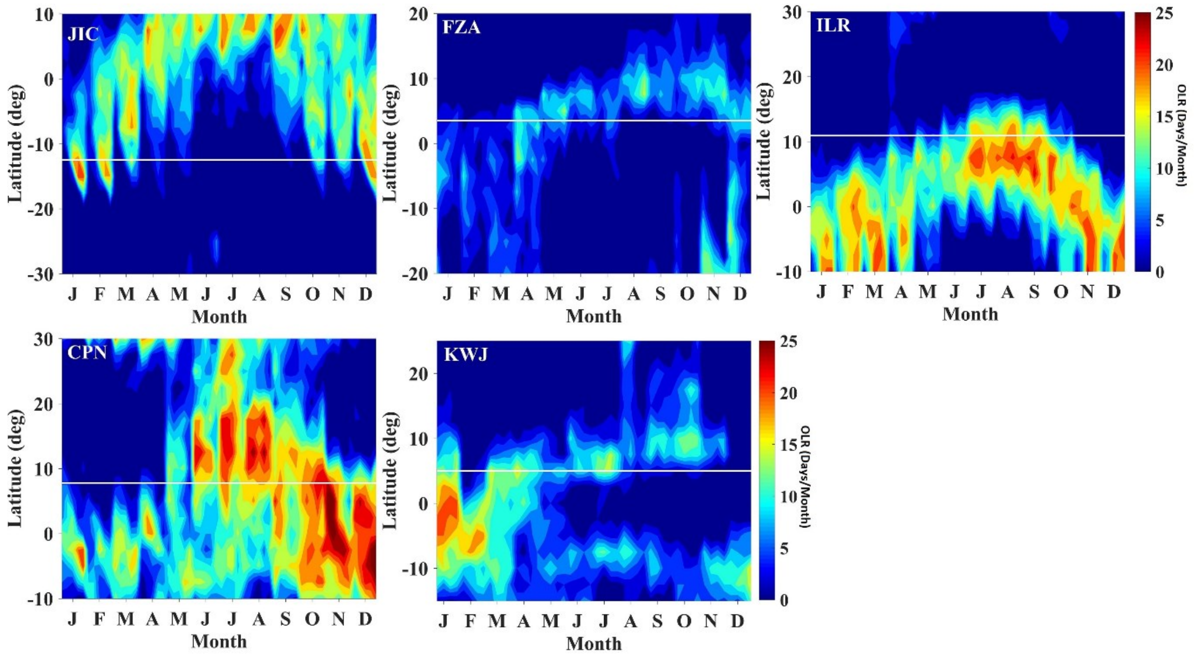

Figure 8: Monthly distribution of the OLR occurrence frequency plotted as a function of the geographic latitude (dip equator indicated by a white line) for each of the stations.

4. Discussion

~~A comparison between our~~The observed~~ation~~ longitudinal variation of the spread F occurrence during the different seasons of both solar epoch have shown a strong similarity ~~and~~ with the earlier ~~investigations~~ studies (Klinngam et al., 2015; Pezzopane et al., 2013; Pietrella et al., 2017; Su et al., 2007; Tsunoda et al., 2015)~~ on the spread F occurrence pattern across these longitudes shows a strong similarity during the different seasons of the MSA and LSA period~~. These ~~previous~~ studies have deployed different measurement techniques to establish a strong linear relationship between the eastward electric field enhancement near the sunset and the seasonal/longitudinal distribution of the spread F occurrence across the solar epoch (Fejer et al., 1999; Huang, 2018; Stolle et al., 2008; Whalen, 2002). ~~The R-T instability mechanism is considered responsible for the plasma irregularity initiation and the observed seasonal variation pattern. This is controlled by the flux tube integrated conductivities of the E and F regions (Σ_F^P and Σ_E^P) and other parameters as shown below (Ossakow, 1981; Sultan, 1996);~~

$$\cancel{\gamma = \frac{\Sigma_F^P}{\Sigma_F^P + \Sigma_E^P} \times \left(\frac{g}{V_{in}} + U_n^p + V_z \right) \times \frac{1}{L} - \beta \qquad (2)}$$

~~Where V_z is the vertical plasma drift component of the $E \times B / B^2$ and U_n^p is the vertical component of the neutral wind perpendicular to the magnetic field. While β is the recombination rate. g is the acceleration due to gravity and V_{in} is the collision frequency.~~

The PRE of the zonal electric field around the local sunset ~~is responsible for the~~ uplift ~~of~~ the F layer into the altitudinal region suitable for the rapid plasma irregularity growth by the R-T instability mechanism. Thus, ~~PRE~~ the vertical drift amplitude was described as ~~a~~ the dominant factor influencing the difference in the observed features such as the onset time, occurrence rate or latitudinal extension of the plasma irregularity across the various season or longitude.

However, other factors such as the zonal drift reversal could also make significant difference in the post-sunset electrodynamics effect on the observed plasma irregularity features across different seasons. ~~An~~For example, ~~of such control is~~ the ~~observed~~ delayed (2 hours lag) ~~in the~~ RSF ~~occurrence~~ onset time during the M-equinox and J-solstice of the LSA compared to the observed characteristics at KWJ during the corresponding seasons of the MSA period ~~at the KWJ station~~ shown in Figures 4 and 5. This is attributed to the delayed ~~in the~~ zonal drift reversal effect on the instability growth rate ~~time and the weaker zonal neutral wind magnitude~~ during the LSA (Su et al., 2009). The eastward reversal of the zonal plasma drift in the upper ionosphere region causes a vertical shear motion and the initiation of the irregularity growth (Kudeki and Bhattacharyya, 1999). ~~As a result of the reduction in the zonal wind and conductivity gradient, which is expected to cause a difference between the near sunset vertical drift~~

~~pattern of the two solar epochs.~~ Su et al., (2009) presented ~~their~~ a theoretical analysis of~~n~~ the zonal drift reversal effect on the post-sunset dynamics at the F region base using the simulation result obtained at the KWJ longitude during the J-solstice season. The zonal drift was expressed as;

$$V_\phi = -\frac{\sigma_H}{\sigma_P}\frac{E_\phi}{B} + U_\phi + \frac{\sigma_H}{\sigma_P}U_p - \frac{J_p}{\sigma_P B} \qquad (1)$$

Where σ_P and σ_H represent the Pedersen and Hall conductivities respectively, $\boldsymbol{B}$ is the magnetic field. $\boldsymbol{E}$, U and J represent the electric field, neutral wind and current respectively, while p and ϕ are the components in the vertical and zonal direction. The average F region altitude near local sunset is above 200 km and $\frac{\sigma_H}{\sigma_P}$ tends toward nil in this altitude range, hence the first and third term in eq.1 are negligible. The zonal drift reversal delay was described as being strongly influenced and indirectly proportional to the flux tube integrated Pedersen conductivity. Hence, an expectedly denser ionosphere and a corresponding increase in the Pedersen conductivity during the MSA will cause an earlier zonal drift reversal and larger occurrence rate as shown in Figure 5. Likewise, the significant difference between the irregularity onsets at both equinoxes could also be as a result of the seasonal variation of the zonal drift reversal. This assumption is due to the disappearance of the RSF onset time delay at KWJ during M-equinox of the MSA as shown in Figure 5. Though~~us~~, further investigation might be required to ~~confirm~~ ascertain that~~whether~~ the same ~~factors~~ phenomenon was ~~were~~ responsible for the ~~significant difference between~~ the delayed onset time ~~observed~~ during the M-equinox seasons of ~~both solar epochs at the~~the LSA. ~~KWJ station as shown in Figure 4(e)~~. ~~On the other hand, the high RSF occurrence percentage at some of the regions during the LSA with a corresponding weak post-sunset PRE indicates a significant contribution by other factors. Though Smith et al., (2016) have attributed such significant RSF occurrence percentage during the LSA to the effect of the requisite PRE threshold for the plasma irregularity initiation being directly dependent on the solar flux index. It was explained that a much lesser PRE peak is required for the uplift of the F region base into a region with reduced ion-neutral collision frequency due to the contracted ionosphere during the LSA period. However, as the density scale length (L) is inversely related to the instability growth rate, we presume that the reduced L during~~

~~LSA is conducive for a faster linear instability growth in response to a strong seeding effect (Huang and Kelley, 1996).~~

The equinox and solstice asymmetry observed in the ~~E~~RSF occurrence percentage at all the longitude regions during both solar epochs appears to be controlled by different mechanisms entirely (Manju and Madhav Haridas, 2015; Tsunoda, 2010c). In the case of the equinox asymmetry, the occurrence percentage is higher during the S-equinox at the JIC, FZA and KWJ stations during the LSA period. While ~~the M-equinox is higher at~~ the CPN ~~station~~ and the ILR stations show~~s~~ approximately ~~the same~~equal occurrence percentage during both equinoctial seasons. The equinox asymmetry is most visible at the Brazilian and Peruvian longitude during the LSA. ~~Most of the regions as shown in~~ Figure 7a~~,~~ shows an approximately equal *h'F* peak at both equinoxes, ~~typically present a deviation between~~which is inconsistent with the observed RSF occurrence ~~percentage~~ asymmetry across these longitudes~~and the approximately equal *h'F* peak at both equinoxes~~ during the LSA. In contrast, the equinoctial asymmetry of the RSF occurrence during the MSA as shown in Figure 7(b). conforms with the corresponding larger *h'F* peak during the M-equinox season at these stations. Manju and Madhav Haridas, (2015) ~~relat~~explored the ~~observation of~~probable relationship between the observed equinox asymmetry in the threshold height ($h'F_c$), ~~and~~the ESF occurrence percentage ~~to the equinox asymmetry in~~and the O/N_2 ratio. This asymmetry was shown to have a strong solar flux dependence. They associated that with a significant difference between the expansions of the thermosphere at both equinoxes as the solar flux increases, which expectedly reflects on the defined $h'F_c$. Th~~e~~is relationship between the thermospheric neutral compositions and the post-sunset dynamics of the F region have also been shown by the earlier studies (Batista et al., 1986; Qian et al., 2009).

The neutral density in the upper thermosphere is known to change with a variation in the O/N_2 ratio, and the post-sunset vertical drift was established to have a directly proportional relationship with the neutral density (Batista et al., 1986; Manju and Madhav Haridas, 2015). Thus, the higher O/N_2 ratio during the M-equinox as reported by Manju and Madhav Haridas, (2015) is expected to correspond to a higher vertical drift peak during this period. Figure 7(b). presents a similar pattern in the estimated PSSR during the equinoctial months. The observed difference in the *h'F* peak is more significant during the MSA, while during the LSA period, the observed PRE peak was approximately equal for both equinoxes across the different regions.~~ This shows a comparably similar pattern with the observed equinoctial asymmetry in the occurrence percentage and duration of RSF for all the regions except in the Brazilian region (represented in Figures 4 and 5).~~ From Figure 4, the Brazilian region recorded a large difference between the occurrence rate of RSF during the equinox seasons of the LSA period. ~~and the higher~~The RSF occurrence percentage was larger during the S-equinox season at the KWJ, JIC and FZA stations. This is attributed to the comparably reduced collision frequency effect on the irregularity growth rate due to the lower neutral density at this season. Consequently, the requisite PRE for irregularity occurrence is smaller than the threshold during M-equinox (Manju and Madhav Haridas, 2015). Hence, the threshold height for RSF occurrence in a season would be dependent on the average neutral density during that season.

The decay of the EEJ current is relatively abrupt during equinox at the large declination angle region and the zonal drift reversal is directly related to the zonal wind reversal as described by Eq.1. In the absence of EEJ dependent factor $(\frac{J_p}{\sigma_P B})$ in Eq.1 will cause the zonal dirft reversal to occur at almost the same time with the zonal wind and yield a strong background condition for the irregularity growth at both equinoxes. However, the sunset time lag tend to change rapidly at the large declination angle region and fig.7c show that it reaches almost twice the peak time lag at the small declination angle during the solstice season. As the sunset time lag increases, the short circuiting effect on the post-sunset F region dynamo persist longer. This implies that the PSSR during the later days of the season will mostly fall below the defined threshold height for RSF occurrence during M-equinox. An unpublished result taken at the FZA station showed that the RSF occurrence percentage reduces from March to April of the same LSA year by ~ 40%. On the other hand, the threshold height during S-equinox is smaller and the rapid change in the sunset time lag would have lesser effect on the irregularity occurrence rate. Hence, the RSF occurrence percentage will be larger during the S-equinox at these longitude regions as described earlier. Coincidentally, the observed equinoctial asymmetry during the LSA seem to be more prevalent at the stations with the larger declination angle. ~~(~~Madhav Haridas et al., (2015) analyzed the role of the sunset time lag on the vertical drift peak in the Indian longitude region during the equinoxes and showed that the partial short circuiting effect persist longer during the LSA and MSA period. In the case of the small declination angle regions, we assume that the larger density during the M-equinox will cause a stronger suppression of the EEJ current effect and an earlier zonal drift reversal time. Thus, the seeding of the R-T instability occurs under a very conducive ionospheric condition for optimal instability growth rate than during the S-equinox. The effect of the fourth term in eq.1 on the difference between the zonal drift at the two equinoxes might become more significant as the asymmetry in the neutral density increases during the MSA (Manju and Madhav Haridas, 2015).

~~On the other hand,~~ The PSSR during the equinoxes show a comparably similar pattern with the observed equinoctial asymmetry in the RSF occurrence percentage for all the regions during MSA except in the Brazilian region (represented in Figures 4 and 5). Where the RSF occurrence percentage peak was approximately ~~the same~~equal for both equinox seasons ~~during the MSA period~~. The American sector has the largest field–aligned Pedersen conductivity and we assume that the significant increase in the conductivity during MSA would nullify the asymmetry in the zonal drift reversal time at this region during equinoxes. On the contrary, this also mean a significant increase in the ionospheric density and the threshold height.~~Furthermore~~ Hence, ~~an~~ the inverse~~anti-~~ solar activity dependence of the RSF occurrence percentage ~~was also~~ observed at the JIC and FZA stations during the S-equinox as shown in ~~Figures~~ Fig. 6(a-b) are attributed to an increased density scale length. ~~Similar anti-solar activity pattern was observed at this longitude region by Su et al., (2008) but less prominent than our result due to the difference in the altitude of data observation. We assume that this resulted from a combined effect of t~~The observed large RSF occurrence percentage during the S-equinox of the LSA ~~in~~ at the~~i~~se longitudes ~~regions during the LSA~~ was earlier related to the effect of the contracted ionospheric density.~~and~~ However, the increase~~d~~ in the bottom-side density scale length during the MSA (Lee, 2010) ~~as compared to the insignificant difference in~~ will increase the threshold PRE for ~~during both epoch~~the irregularity occurrence (Smith et al., 2016). The inconsisten~~tcy in the~~ equinoctial asymmetry pattern at different solar flux index was also observed in the Atlantic region during the study of the global equatorial plasma bubble occurrence (Gentile et al., 2006). Similar inverse solar activity pattern was observed at this longitude region by Su et al., (2007)) as shown in their Fig. 3b but less prominent than our result due to the difference in the altitude of data observation.

During the solstice seasons, the observed asymmetry in the PRE of the F layer and the RSF occurrence percentage at the low declination angle longitudes are inconsistent with the corresponding sunset time lag. Unlike the FZA and KWJ stations where the asymmetry between the solstices could be explained by the difference in the sunset time lag, the~~se~~ other three ~~longitudes~~ Ionosonde stations have approximately the same sunset time lag at both solstices. The results showed larger RSF occurrence percentage during the D-solstice at these longitudes. The significant asymmetry in the ionospheric density distribution during the solstice seasons is considered as a probable factor in this case. There is post-sunset EEJ current due to large sunset time lag during the solstice seasons, which strongly affects the instability growth rate. The larger density during D-solstice indicates an earlier zonal drift reversal and a more conducive ionospheric condition for the seeding of the R-T instability process (Su et al., 2009).

In a similar discussion, ~~(~~Tsunoda, (2010a) has attributed the observed asymmetry in the RSF occurrence during the solstices to the seasonal variation of the convective gravity wave (GW) sources at these longitudes and suggested the GW phase front and magnetic field line alignment (GWBA) hypothesis. This has been discussed extensively discussed by previous studies (Li et al., 2016; Su et al., 2014; Tsunoda, 2010a) but further analysis are considered necessary to substantiate the correlation between the seasonal distribution of GW and RSF occurrence across these longitudes. However, the presence of a large GW amplitude is widely considered as a requisite condition for the generation of spread F under a weak background ionospheric condition (Abdu et al., 2009; Manju et al., 2016). There are frequent GW occurrence recorded in the Asian and African regions (Su et al., 2014) and the seeding effect is expected to have played a significant role in the observed plasma irregularity generation in this regions. Apart from the requisite GW and $\vec{B}$ alignment, a large local electron density was described as an important prerequisite for the large ESF growth (Krall et al., 2013b). The large electron density is considered necessary to support the GW induced electric field and the plasma instability growth. Coincidentally, the peak electron density in both regions (unpublished result) shows similar seasonal variation with the RSF occurrence percentage during LSA. Though, these plasma irregularities will be confined mostly to the low altitude region during this period, especially in the Asian region. The weak PRE at CPN results from the large magnetic field strength and a small field line integrated conductivities at this longitude sector. Under such circumstance, the GW induced perturbation electric field might be suppressed and reduced impact on the instability growth across these longitudes in spite of the large GW frequency. Kil and Heelis, (1998) suggested that the longitudinal distribution of the ESF occurrence is dependent on the height of observation and the occurrence probability at the low altitude was related to the seed perturbation from tropospheric source.

Hence, we discuss the probable role of GW in the recorded ESF occurrence percentage, especially during the LSA. The seeding effect is considered an important parameter in the analysis of the plasma irregularity generation during days characterized by a weak ambient ionospheric condition as observed across most regions. A direct link was established between the GW from the intertropical convergence zone (ITCZ) and the frequency of ESF activity using the outgoing longwave radiation (OLR) data (Ogawa et al., 2006; Tsunoda, 2010c). The seeding of the ionospheric density perturbation is expected to occur when the ITCZ is located near the dip equator (Tsunoda, 2010a). Which raised a discussion about the GW phase front and magnetic field line alignment (GWBA) hypothesis. The GW induced zonal electric field in the presence of the background density gradient enhances the plasma instability growth along that longitude. This mechanism combined with the STBA theory was considered important to form a complete description of the seasonal morphology of ESF occurrence across different longitude (Tsunoda, 2010a). ~~The geographic map of the OLR measurement provides the longitudinal distribution of the deep convective activity (Gu and Zhang, 2002; Waliser and Gautier, 1993). The seasonal variation of the GW occurrence across the different regions will then be analyzed using the interpolated OLR data that are available from the National Oceanic and Atmospheric Administration NOAA website (http://www.esrl.noaa.gov/psd/data/gridded/data.interp_OLR.html). Which will be compared with the observed seasonal variation of the ESF occurrence percentage across these regions.~~

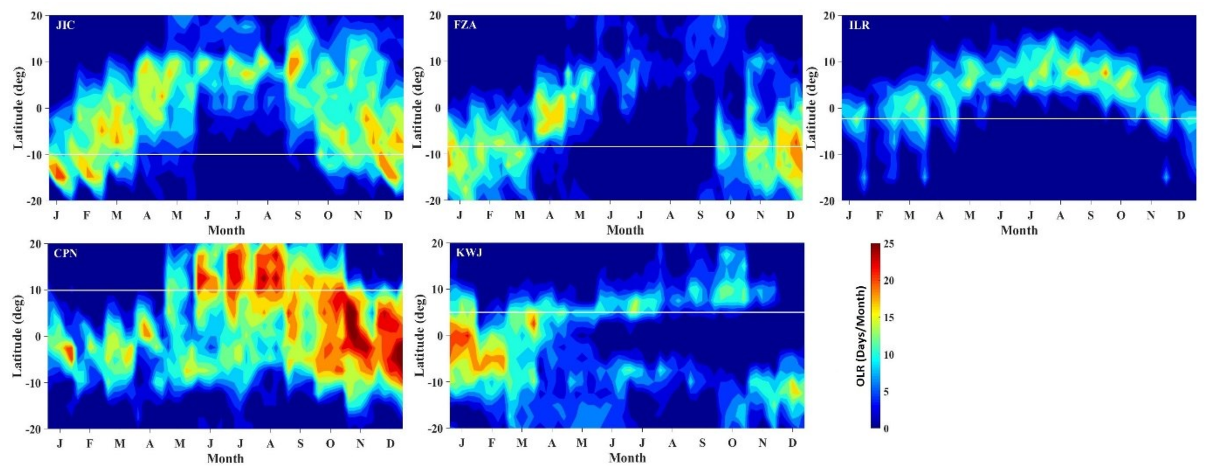

~~Figure 8: Monthly distribution of the OLR occurrence frequency plotted as a function of the geographic latitude (dip equator indicated by a white line) for each of the stations.~~

~~There has been an extensive discussion on the geometry and coupling of the upward propagating GW considered most suitable for the ESF initiation (Krall et al., 2013a; Tsunoda, 2010c, 2010b). The seeding of plasma irregularity is expected to occur when the phase front of the GW becomes aligned with the magnetic field line ($\vec{B}$). This alignment condition is considered possible, only if the convective active regions are located close to the magnetic dip equator (Tsunoda, 2010a). Figure 8. shows the variation of the monthly averaged OLR distribution across the five stations. With the measurement taken over 10 degrees longitudinal range which brackets the location of the ionosonde station and ± 20 degrees at both sides of the dip equator (white line). The defined threshold OLR strength used to distinguish regions of convective and non-convective activity was 200 W/m^2 in each bin per day (Gu and Zhang, 2002). The frequency of the OLR occurrences represents the frequency of the GW occurrences in each month. In the regions where the dip equator is located at the southern hemisphere, we noticed that the GW occurrence peak during the J-solstice is located farther from the dip equator compared to the D-solstice. The observed pattern of the monthly GW distribution displayed a tendency to produce a solstitial asymmetry in the expected seeding effect on the ESF occurrence. On the other hand, a large OLR occurrence frequency was observed close to the dip equator from January to November at the KWJ longitude. While throughout the year, a varying degree of large OLR occurrence was observed around the dip equator at the CPN longitude. A comparison between the OLR occurrence~~

~~frequency and the RSF occurrence percentage (Figure 4) shows a strong agreement at all the longitudes except the CPN station. Where the observed low RSF occurrence percentage contradicts the large OLR frequency around the dip equator in the region.~~

~~Apart from the requisite GW and $\vec{B}$ alignment, a large local electron density was also described as an important prerequisite for the large ESF growth (Krall et al., 2013b). The large electron density is considered necessary to support the GW induced electric field and the plasma instability growth. The relationship between the perturbation wind and the induced electric field is expressed as (Abdu et al., 2009; Tsunoda, 2010c);~~

$$\cancel{\delta \boldsymbol{J} = \sigma_p(\delta \boldsymbol{E} + \delta \boldsymbol{U} \times \boldsymbol{B}) = 0} \qquad \cancel{(3)}$$

$$\cancel{\delta \boldsymbol{E} = -(\delta \boldsymbol{U} \times \boldsymbol{B})} \qquad \cancel{(4)}$$

~~Where σ_p is the Pedersen conductivity, $\delta \boldsymbol{U}$ is the perturbation wind velocity due to gravity wave, $\delta \boldsymbol{E}$ is the perturbation electric field and $\boldsymbol{B}$ is the magnetic field. The total electric field is assumed to be a sum of the ambient and perturbation electric field. In the absence of the ambient electric field, the vertical velocity drift induced by the perturbation $\boldsymbol{E}$ field can be expressed as $V = {}^{v_{in}}/_{\Omega}\left({}^{\delta \boldsymbol{E}}/_{\boldsymbol{B}}\right)$.~~

The average RSF occurrence percentage observed at the ILR station was greater than 80% by 21:00 LT during these seasons except J-solstice, which has 60% and significantly larger than the other longitudes. Similarly~~In the case of the West African sector~~, past studies (Okoh et al., 2017; Yizengaw et al., 2013) have ~~presented a similar~~ discussed~~ion about~~ the role of GW in the observed large RSF occurrence during ~~a~~ the solstice months. ~~Yizengaw et al., (2013) attributed the post-midnight enhancement of the eastward polarization electric field in the West African region to the presence of the localized charged particle. These dust particles are generated by the strong gusty wind that characterizes the harmattan season in the region. The particles are dispersed into higher altitude, where the associated friction becomes the source of the polarized electric charges and subsequently enhances zonal E field. Thus, the perturbation electric field further increases the vertical plasma vortex flow in the evening ionosphere and the subsequent initiation of the R-T instability process.~~ The RSF occurrence on the ionogram before 21:00 LT was assumed as the locally generated irregularity (Manju et al., 2016). The large occurrence percentage of the locally generated RSF at ILR shows a considerable correlation with the frequent OLR occurrence across the different months. Especially during the solstice seasons of the LSA, considering that this period is usually characterized by a weak PRE vertical drift (mostly < 20m/s) and the small declination angle, the seeding effect is expected to have played a significant role in the observed plasma irregularity generation. These plasma irregularities will be restricted mostly to the low altitude region. ~~(~~Kil and Heelis, (1998) suggested that the longitudinal distribution of the ESF occurrence is dependent on the height of observation and the occurrence probability at the low altitude was related to the seed perturbation from tropospheric source. The presence of a ~~more~~ frequent~~ly~~ active ITCZ is expected to enhance the plasma irregularity seeding in a region (Li et al., 2016). This complementary role of the GW induced zonal E field and the observed monthly distribution pattern of the convective region is found to be consistent with the solstice asymmetry in the ESF occurrence. ~~Such a similar mechanism~~The same analogy is expected to be applicable to the other four longitudinal sectors during seasons where intense convective activity is observed near the magnetic dip equator. ~~However, considering the negative correlation between the OLR frequency and RSF occurrence at the CPN station.~~ ~~(~~Li et al., (2016) have suggested that the analysis of the comparison between the locally generated ESF and the OLR frequency data averaged over a small longitude range ($\pm 5^0$) will yield a larger correlation coefficient than the observation in the earlier study (Su et al., 2014). However, Figure 8 shows a large OLR frequency at CPN during the LSA, which is contrary to the monthly mean of the RSF occurrence percentage of the corresponding months. Hence, we ~~highlight~~ are considering the effect of the ambient F region electrodynamics on the seeding of the plasma irregularity ~~in the Asian~~these sectors.

In order to analyze the relationship between the OLR measurement and the irregularity generation, it is important to also consider the ionospheric electro-dynamical effect in that region. Apart from the requisite GW and $\vec{B}$ alignment, a large local electron density was ~~also~~ described as an important prerequisite for the large ESF growth (Krall et al., 2013b). The large electron density is considered necessary to support the GW induced electric field and the plasma instability growth. Figure 4 of Vichare and Richmond, (2005) presented a zonal variation of PRE in comparison with the magnetic field strength, field line integrated Pedersen conductivity and zonal E field. The ~~weakest~~ zonal variation of PRE ~~were~~ is relatively small across~~recorded in~~ the longitudinal range 90ºE – 120ºE and 160ºE – 240ºE, which encloses the CPN and KWJ stations respectively. The ~~recorded~~ weak PRE ~~in the~~at CPN~~former longitude sector could be attributed to~~results from the ~~combined effect of~~ large magnetic field strength and a small field line integrated conductivities at this longitude sector. While, the zonal E field ~~later longitude range~~ was shown to have the minimum ~~zonal E field, which correlates with~~ value at the KWJ longitude region and consequently the generally weak PSSR observed ~~in~~ at these regions during the LSA (Figure 7b.). Under such circumstance, the GW induced perturbation electric field might have negligible impact on the instability growth across these longitudes in spite of the large OLR frequency. Hence, the negative ~~or weak~~ correlation observed ~~in~~ between the OLR frequency and the RSF occurrence percentage at both sectors is associated with the unfavourable background ionospheric condition for the plasma irregularity growth. It is also ~~important to~~ noteworthy that the observed solstitial asymmetry in ESF occurrence becomes more prominent at the CPN station during the MSA, which correlates with an expected significant increase in the local electron density. Likewise, the observed significant increase in the ~~ESF~~ RSF occurrence percentage ~~increases significant~~ at the KWJ during the J-solstice, which is uncorrelated with the percentage increase ~~of~~ in the PSSR ~~in relation to the solar flux dependence~~during the corresponding season as shown in Figure 7b. These are considered as an evidence of improved seeding of the plasma instability growth ~~triggered by a~~as a result of the substantial increase in the local electron density during the MSA.

5. Conclusion

The statistical result of the hourly variation of the RSF occurrence percentage across different longitude sectors was investigated during the MSA and LSA period for stations close to the magnetic equator. The manual observation of the seasonal variation of the RSF occurrence pattern using the ionogram data revealed the distinct RSF occurrence features at each of the regions. This highlighted the complex morphology of the ESF events and the diverse role of the different factors contributing to plasma irregularity initiation across the different longitudes during the MSA and LSA. The West African region (ILR) has the highest average ESF occurrence percentage across the four seasons during the LSA period, even when the ambient ionospheric condition is less conducive for the R-T instability growth.

Other important observations included the varying longitudinal pattern of the equinox asymmetry during the LSA and MSA. The probable role of the zonal drift reversal time was associated with the observed inconsistency in the asymmetry pattern ~~requires further investigation to understand the factors responsible for the changes~~ during the equinoctial season ~~maximum during the different~~ of both solar epochs. Likewise, an anti-solar activity variation of the ESF occurrence percentage was also observed at the JIC and FZA stations during the S-equinox. This was attributed to the possible role of an expected increase in the bottom-side density scale length with the solar flux index. ~~Finally, the observed solstice asymmetry in the low declination angle region and the PRE peak deviation from the expected STBA ratio were associated with the presence of a strong convective activity around the dip equator. The described GWBA theory proved to be a sufficient explanation for the observed discrepancy in the seasonal variation of ESF occurrence in relation with the STBA theory. Hence, the seed perturbation effect was considered as an important factor enhancing the plasma irregularity growth during unfavourable ambient ionospheric condition.~~

Acknowledgement

References

Abdu, M.A., 2016. Electrodynamics of ionospheric weather over low latitudes. Geosci. Lett. 3, 11. doi:10.1186/s40562-016-0043-6

Abdu, M.A., 2001. Outstanding problems in the equatorial ionosphere-thermosphere electrodynamics relevant to spread F. J. Atmos. Solar-Terrestrial Phys. 63, 869–884. doi:10.1016/S1364-6826(00)00201-7

Abdu, M.A., Alam Kherani, E., Batista, I.S., De Paula, E.R., Fritts, D.C., Sobral, J.H.A., 2009. Gravity wave initiation of equatorial spread F/plasma bubble irregularities based on observational data from the SpreadFEx campaign. Ann. Geophys. 27, 2607–2622. doi:10.5194/angeo-27-2607-2009

Abdu, M.A., Batista, I.S., Sobral, J.H.A., 1992. A New Aspect of Magnetic Declination Control of Equatorial Spread F and F Region Dynamo. J. Geophys. Res. Sp. Phys. 97, 14,897-14,904. doi:10.1029/92JA00826

Abdu, M.A., Bittencourt, J.A., Batista, I.S., 1981. Magnetic declination control of the equatorial F region dybamo electric field development and spread F. Jgr 86, 143–1446. doi:10.1029/JA086iA13p11443

Aveiro, H.C., Denardini, C.M., Abdu, M.A., 2009. Climatology of gravity waves-induced electric fields in the equatorial E region. J. Geophys. Res. Sp. Phys. doi:10.1029/2009JA014177

Balan, N., Liu, L., Le, H., 2018. A brief review of equatorial ionization anomaly and ionospheric irregularities. Earth Planet. Phys. doi:10.26464/epp2018025

Basu, S., Basu, S., Aarons, J., McClure, J.P., Cousins, M.D., 1978. ON THE COEXISTENCE OF KILOMETER- AND METER-SCALE IRREGULARITIES IN THE NIGHTTIME EQUATORIAL F REGION. J Geophys Res 83, 4219–4226. doi:10.1029/JA083iA09p04219

Batista, I.S., Abdu, M.A., Bittencourt, J.A., 1986. Equatorial F region vertical plasma drifts: Seasonal and longitudinal asymmetries in the American sector. J. Geophys. Res. Sp. Phys. 91, 12055–12064. doi:10.1029/JA091iA11p12055

Booker, H.G., Wells, H.W., 1938. Scattering of radio waves by the F -region of the ionosphere. J. Geophys. Res. 43, 249. doi:10.1029/TE043i003p00249

Bowman, G. G., 1960. A relationship between “spread-F” and the height of the F2 ionospheric layer. Aust. J. Phys. 13, 69–72. doi:10.1071/PH600069

Bowman, G.G., 1998. Short-term delays (hours) of ionospheric spread F occurrence at a range of latitudes, following geomagnetic activity. J. Geophys. Res. Atmos. doi:10.1029/98JA00630

Bowman, G.G., 1990. A review of some recent work on mid-latitude spread-F occurence as detected by ionosondes. J. Geomag. Geoelectr. 42, 109–138.

Candido, C.M.N., Batista, I.S., Becker-Guedes, F., Abdu, M.A., Sobral, J.H.A., Takahashi, H., 2011. Spread F occurrence over a southern anomaly crest location in Brazil during June solstice of solar minimum activity. J. Geophys. Res. Sp. Phys. doi:10.1029/2010JA016374

Dabas, R.S., Singh, L., Lakshmi, D.R., Subramanyam, P., Chopra, P., Garg, S.C., 2003. Evolution and dynamics of equatorial plasma bubbles: Relationships to ExB drift, postsunset total electron content enhancements, and equatorial electrojet strength. Radio Sci. 38, n/a-n/a. doi:10.1029/2001RS002586

Dao, T., Otsuka, Y., Shiokawa, K., Nishioka, M., Yamamoto, M., Buhari, S.M., Abdullah, M., Husin, A., 2017. Coordinated observations of postmidnight irregularities and thermospheric neutral winds and temperatures at low latitudes. J. Geophys. Res. Sp. Phys. doi:10.1002/2017JA024048

De Paula, E.R., Muella, M.T.A.H., Sobral, J.H.A., Abdu, M.A., Batista, I.S., Beach, T.L., Groves, K.M., 2010. Magnetic conjugate point observations of kilometer and hundred-meter scale irregularities and zonal drifts. J. Geophys. Res. Sp. Phys. 115. doi:10.1029/2010JA015383

Eccles, J. V., St. Maurice, J.P., Schunk, R.W., 2015. Mechanisms underlying the prereversal enhancement of the vertical plasma drift in the low-latitude ionosphere. J. Geophys. Res. Sp. Phys. 120, 4950–4970. doi:10.1002/2014JA020664

Fejer, B.G., Scherliess, L., de Paula, E.R., 1999. Effects of the vertical plasma drift velocity on the generation and evolution of equatorial spread F. J. Geophys. Res. Sp. Phys. 104, 19859–19869. doi:10.1029/1999JA900271

Gentile, L.C., Burke, W.J., Rich, F.J., 2006. A global climatology for equatorial plasma bubbles in the topside ionosphere. Ann. Geophys. 24, 163–172. doi:10.5194/angeo-24-163-2006

Gu, G., Zhang, C., 2002. Cloud components of the Intertropical Convergence Zone. J. Geophys. Res. Atmos. doi:10.1029/2002JD002089

Haldoupis, C., Kelley, M.C., Hussey, G.C., Shalimov, S., 2003. Role of unstable sporadic-E layers in the generation of midlatitude spread F. J. Geophys. Res. Sp. Phys. doi:10.1029/2003JA009956

Heelis, R.A., 2004. Electrodynamics in the low and middle latitude ionosphere: A tutorial. J. Atmos. Solar-Terrestrial Phys. 66, 825–838. doi:10.1016/j.jastp.2004.01.034

Hoang, T.L., Abdu, M.A., MacDougall, J., Batista, I.S., 2010. Longitudinal differences in the equatorial spread F characteristics between Vietnam and Brazil. Adv. Sp. Res. 45, 351–360. doi:10.1016/j.asr.2009.08.019

Huang, C.S., 2018. Effects of the postsunset vertical plasma drift on the generation of equatorial spread F. Prog. Earth Planet. Sci. 5. doi:10.1186/s40645-017-0155-4

Huang, C.S., 2017. The characteristics and generation mechanism of small-amplitude and large-amplitude ESF irregularities observed by the C/NOFS satellite. J. Geophys. Res. Sp. Phys. 122, 8959–8973. doi:10.1002/2017JA024041

Kil, H., Heelis, R.A., 1998. Global distribution of density irregularities in the equatorial ionosphere. J. Geophys. Res. Sp. Phys. doi:10.1029/97ja02698

Klinngam, S., Supnithi, P., Rungraengwajiake, S., Tsugawa, T., Ishii, M., Maruyama, T., 2015. The occurrence of equatorial spread-F at conjugate stations in Southeast Asia. Adv. Sp. Res. 55, 2139–2147. doi:10.1016/j.asr.2014.10.003

Krall, J., Huba, J.D., Fritts, D.C., 2013a. On the seeding of equatorial spread F by gravity waves. Geophys. Res. Lett. 40, 661–664. doi:10.1002/grl.50144

Krall, J., Huba, J.D., Joyce, G., Hei, M., 2013b. Simulation of the seeding of equatorial spread F by circular gravity waves. Geophys. Res. Lett. 40, 1–5. doi:10.1029/ 2012GL054022

Kudeki, E., Bhattacharyya, S., 1999. Postsunset vortex in equatorial F -region plasma drifts and implications for bottomside spread- F. J. Geophys. Res. Sp. Phys. doi:10.1029/1998JA900111

Lee, C.C., 2010. Occurrence and onset conditions of postsunset equatorial spread F at Jicamarca during solar minimum and maximum. J. Geophys. Res. Sp. Phys. 115, 1–7. doi:10.1029/2010JA015650

Lee, C.C., Liu, J.Y., Reinisch, B.W., Chen, W.S., Chu, F.D., 2005. The effects of the pre-reversal ExB drift, the EIA asymmetry, and magnetic activity on the equatorial spread F during solar maximum. Ann. Geophys. 23, 745–751. doi:10.5194/angeo-23-745-2005

Li, G., Ning, B., Liu, L., Ren, Z., Lei, J., Su, S.-Y., 2008. The correlation of longitudinal/seasonal variations of evening equatorial pre-reversal drift and of plasma bubbles, in: Annales Geophysicae. pp. 2571–2578.

Li, G., Otsuka, Y., Ning, B., Abdu, M.A., Yamamoto, M., Wan, W., Liu, L., Abadi, P., 2016. Enhanced ionospheric plasma bubble generation in more active ITCZ. Geophys. Res. Lett. doi:10.1002/2016GL068145

Madhav Haridas, M.K., Manju, G., Pant, T.K., 2015. On the solar activity variations of nocturnal F region vertical drifts covering two solar cycles in the Indian longitude sector. J. Geophys. Res. Sp. Phys. doi:10.1002/2014JA020561

Manju, G., Madhav Haridas, M.K., 2015. On the equinoctial asymmetry in the threshold height for the occurrence of equatorial spread F. J. Atmos. Solar-Terrestrial Phys. 124, 59–62. doi:10.1016/j.jastp.2015.01.008

Manju, G., Madhav Haridas, M.K., Aswathy, R.P., 2016. Role of gravity wave seed perturbations in ESF day-to-day variability: A quantitative approach. Adv. Sp. Res. 57, 1021–1028. doi:10.1016/j.asr.2015.12.019

Maruyama, T., Matuura, N., 1984. Longitudinal variability of annual changes in activity of equatorial spread *F* and plasma bubbles. J. Geophys. Res. 89, 10903. doi:10.1029/JA089iA12p10903

Maruyama, T., Saito, S., Kawamura, M., Nozaki, K., 2008. Thermospheric meridional winds as deduced from ionosonde chain at low and equatorial latitudes and their connection with midnight temperature maximum. J. Geophys. Res. Sp. Phys. 113, 1–9. doi:10.1029/2008JA013031

Miller, C.A., 1997. Electrodynamics of midlatitude spread F 2. a new theory of gravity wave electric fields. J. Geophys. Res. A Sp. Phys. doi:10.1029/96JA03840

Narayanan, V.L., Sau, S., Gurubaran, S., Shiokawa, K., Balan, N., Emperumal, K., Sripathi, S., 2014. A statistical study of satellite traces and evolution of equatorial spread F. Earth, Planets Sp. 66, 1. doi:10.1186/s40623-014-0160-4

Ogawa, T., Otsuka, Y., Shiokawa, K., Saito, A., Nishioka, M., 2006. Ionospheric disturbances over Indonesia and their possible association with atmospheric gravity waves from the troposphere. J. Meteorol. Soc. JAPAN. doi:10.2151/jmsj.84A.327

Okoh, D., Rabiu, B., Shiokawa, K., Otsuka, Y., Segun, B., Falayi, E., Onwuneme, S., Kaka, R., 2017. First Study on the Occurrence Frequency of Equatorial Plasma Bubbles over West Africa Using an All-Sky Airglow Imager and GNSS Receivers. J. Geophys. Res. Sp. Phys. 122, 12430–12444. doi:10.1002/2017JA024602

Otsuka, Y., 2018. Review of the generation mechanisms of post-midnight irregularities in the equatorial and low-latitude ionosphere. Prog. Earth Planet. Sci. doi:10.1186/s40645-018-0212-7

Pezzopane, M., Zuccheretti, E., Abadi, P., De Abreu, A.J., De Jesus, R., Fagundes, P.R., Supnithi, P., Rungraengwajiake, S., Nagatsuma, T., Tsugawa, T., Cabrera, M.A., Ezquer, R.G., 2013. Low-latitude equinoctial spread-F occurrence at different longitude sectors under low solar activity. Ann. Geophys. 31, 153–162. doi:10.5194/angeo-31-153-2013

Pietrella, M., Pezzopane, M., Fagundes, P.R., Jesus, R. De, Supnithi, P., Klinngam, S., Ezquer, R.G., Cabrera, M.A., 2017. Journal of Atmospheric and Solar-Terrestrial Physics Equinoctial spread-F occurrence at low latitudes in different longitude sectors under moderate and high solar activity. J. Atmos. Solar-Terrestrial Phys. 164, e815–e818. doi:10.1016/j.jastp.2017.07.007

Qian, L., Solomon, S.C., Kane, T.J., 2009. Seasonal variation of thermospheric density and composition. J. Geophys. Res. Sp. Phys. 114. doi:10.1029/2008JA013643

Reinisch, B.W., I. A. Galkin, 2011. Global ionospheric radio observatory (GIRO). Earth, Planets Sp. 63, 377–381. doi:10.5047/eps2011.03.001.2011

Sastri, J.H., Ranganath Rao, H.N., Somayajulu, V. V., Chandra, H., 1994. Thermospheric meridional neutral winds associated with equatorial midnight temperature maximum (MTM). Geophys. Res. Lett. doi:10.1029/93GL03009

Seif, A., Tsunoda, R.T., Abdullah, M., Hasbi, A.M., 2015. Daytime gigahertz scintillations near magnetic equator: Relationship to blanketing sporadic e and gradient-drift instability. Earth, Planets Sp. doi:10.1186/s40623-015-0348-2

Shi, J.K., Wang, G.J., Reinisch, B.W., Shang, S.P., Wang, X., Zherebotsov, G., Potekhin, A., 2011. Relationship between strong range spread F and ionospheric scintillations observed in Hainan from 2003 to 2007. J. Geophys. Res. Sp. Phys. 116, 1–5. doi:10.1029/2011JA016806

Smith, J.M., Rodrigues, F.S., Fejer, B.G., Milla, M.A., 2016. Coherent and incoherent scatter radar study of the climatology and day-to-day variability of mean F region vertical drifts and equatorial spread F. J. Geophys. Res. A Sp. Phys. 121, 1466–1482. doi:10.1002/2015JA021934

Stolle, C., Lür, H., Fejer, B.G., 2008. Relation between the occurrence rate of ESF and the equatorial vertical plasma drift velocity at sunset derived from global observations. Ann. Geophys. 26, 3979–3988. doi:10.5194/angeo-26-3979-2008

Stoneback, R.A., Heelis, R.A., Burrell, A.G., Coley, W.R., Fejer, B.G., Pacheco, E., 2011. Observations of quiet time vertical ion drift in the equatorial ionosphere during the solar minimum period of 2009. J. Geophys. Res. Sp. Phys. doi:10.1029/2011JA016712

Su, S.-Y., Chao, C.K., Liu, C.H., 2008. On monthly/seasonal/longitudinal variations of equatorial irregularity occurrences and their relationship with the postsunset vertical drift velocities. J. Geophys. Res. Sp. Phys. 113.

Su, S.Y., Chao, C.K., Liu, C.H., 2009. Cause of different local time distribution in the postsunset equatorial ionospheric irregularity occurrences between June and December solstices. J. Geophys. Res. Sp. Phys. 114. doi:10.1029/2008JA013858

Su, S.Y., Chao, C.K., Liu, C.H., Ho, H.H., 2007. Meridional wind effect on anti-solar activity correlation of equatorial density irregularity distribution. J. Geophys. Res. Sp. Phys. 112, 1–11. doi:10.1029/2007JA012261

Su, S.Y., Wu, C.L., Liu, C.H., 2014. Correlation between the global occurrences of ionospheric irregularities and deep atmospheric convective clouds in the intertropical convergence zone (ITCZ). Earth, Planets Sp. doi:10.1186/1880-5981-66-134

Tsunoda, R.T., 2010a. On equatorial spread F: Establishing a seeding hypothesis. J. Geophys. Res. Sp. Phys. 115. doi:10.1029/2010JA015564

Tsunoda, R.T., 2010b. On seeding equatorial spread F: Circular gravity waves. Geophys. Res. Lett. 37. doi:10.1029/2010GL043422

Tsunoda, R.T., 2010c. On seeding equatorial spread F during solstices. Geophys. Res. Lett. doi:10.1029/2010GL042576

Tsunoda, R.T., 1985. Control of the seasonal and longitudinal occurrence of equatorial scintillations by the longitudinal gradient in integrated Eregion Pedersen conductivity. JGR 90, 447–456. doi:10.1029/JA090iA01p00447

Tsunoda, R.T., Nguyen, T.T., Le, M.H., 2015. Effects of tidal forcing, conductivity gradient, and active seeding on the climatology of equatorial spread F over Kwajalein. J. Geophys. Res. Sp. Phys. 120, 632–653. doi:10.1002/2014JA020762

Vichare, G., Richmond, A.D., 2005. Simulation study of the longitudinal variation of evening vertical ionospheric drifts at the magnetic equator during equinox. J. Geophys. Res. Sp. Phys. 110, 1–8. doi:10.1029/2004JA010720

Waliser, D.E., Gautier, C., 1993. A satellite-derived climatology of the ITCZ. J. Clim. doi:10.1175/1520-0442(1993)006<2162:ASDCOT>2.0.CO;2

Wang, G.J., Shi, J.K., Wang, Z., Wang, X., Romanova, E., Ratovsky, K., Polekh, N.M., 2017. Solar cycle variation of ionospheric parameters over the low latitude station Hainan, China, during 2002–2012 and its comparison with IRI-2012 model. Adv. Sp. Res. 60, 381–395. doi:10.1016/j.asr.2016.12.013

Whalen, J.A., 2002. Dependence of equatorial bubbles and bottomside spread F on season, magnetic activity, and e ?? B drift velocity during solar maximum. J. Geophys. Res. Sp. Phys. 107. doi:10.1029/2001JA000039

Woodman, R.F., La Hoz, C., 1976. RADAR OBSERVATIONS OF F REGION EQUATORIAL IRREGULARITIES. J Geophys Res 81, 5447–5466. doi:10.1029/JA081i031p05447

Yizengaw, E., Retterer, J., Pacheco, E.E., Roddy, P., Groves, K., Caton, R., Baki, P., 2013. Postmidnight bubbles and scintillations in the quiet-time June solstice. Geophys. Res. Lett. 40, 5592–5597. doi:10.1002/2013GL058307